causes the release of cytochrome C from mitochondria, which activates the apoptotic caspase cascade.[1,8] Anti-cancer drugs, γ-irradiation, and factor deprivation can activate this death machinery. On the other hand, when cytotoxic T lymphocytes (CTLs) and natural killer (NK) cells attack their target cells, they often use the extrinsic pathway, in which the target cells' death machinery is activated via death factors (Fas ligand, tumor necrosis factor [TNF], and TNF-related apoptosis-inducing factor [TRAIL]).[9] In both the extrinsic and intrinsic pathways, a cascade of cysteine proteases (caspases) is activated, which cleave more than 300 specific substrates.[10,11] This leads to the biochemical and morphological changes that are characteristic of apoptosis, including the fragmentation of chromosomal DNA, the blebbing of the plasma membrane, and the exposure of phosphatidylserine on the cell surface.

Erythropoiesis

Red blood cells are produced in the yolk sac (primitive erythropoiesis) in early mammalian embryogenesis.[12] The location of erythropoiesis shifts to the fetal liver late in embryogenesis and to the bone marrow after birth. The erythropoiesis in the fetal liver and bone marrow is called "definitive erythropoiesis."[12] The cells produced in the yolk sac by primitive erythropoiesis contain nuclei, but the one produced in the fetal liver and bone marrow do not. Within the fetal liver and bone marrow, definitive erythropoiesis takes place at anatomical entities called erythroblastic islands.[13,14] A single macrophage, to which erythroblasts bind, lies at the center of each island. The erythroblasts proliferate, differentiate, and expel their nucleus while bound to the macrophage.

During definitive erythropoiesis, transcription factors such as GATA-1, EKLF, NF-E2, and TAL-1 induce the expression of erythroid-specific genes, such as the α- and β-globin genes,[15] and at the final stage of erythropoiesis, the erythroblasts expel their nucleus. Each expelled nucleus is covered by a plasma membrane and connected to the reticulocyte by a thin membranous material,[16] suggesting that this process is a type of asymmetrical cell division. A weak physical stress in the bone marrow, such as shear stress, which is the tangential component of hemodynamic forces, is sufficient to separate the nucleus from its reticulocyte.

Engulfment of apoptotic cells and nuclei from erythroid precursors

Phagocytes engulf and clear large numbers of dead cells and nuclei daily, including 10^{10} neutrophils (as mentioned earlier), and more than 1.0×10^{12} nuclei expelled from erythroblasts during erythropoiesis. The cells responsible for clearing the dead cells and nuclei are mainly professional phagocytes such as macrophages and immature dendritic cells (DCs). Fibroblasts and epithelial cells also engulf dead cells, in particular in animals that do not have macrophages or when macrophages have not yet developed, early in mammalian embryogenesis. However, compared with the professional phagocytes, the ability of fibroblasts and epithelial cells to engulf dead cells seems to be low,[17] and the machinery used by these cells may be different from that of the professional phagocytes.

As soon as cells undergo apoptosis, macrophages approach the dead cells, recognize them as dead, and engulf them,[5] but they do not engulf healthy living cells, suggesting that the apoptotic cells present an "eat me" signal to phagocytes. Various molecules have been proposed as an "eat me" signal.[18] Among them, phosphatidylserine, a glycero-phospholipid is one of the strongest candidates[19] (Fig. 1).

Phosphatidylserine

Phosphatidylserine is usually kept on the inner leaflet of the plasma membrane, by the action of an ATP-dependent translocase or flippase.[20] Some members of the type IV P-type ATPase (P4-ATPase) family have been identified as a specific flippase(s) of phosphatidylserine.[21] Other enzymes that regulate the distribution of phospholipids are ATP-dependent floppases and Ca-dependent scramblases. Floppases specifically transport phosphatidylserine from the inner to the outer leaflet of the plasma membrane, while scramblases non-selectively catalyze bidirectional transport of phospholipids between the leaflets.[20] Members of the ABC-transporter family have been proposed as floppases, but ABCA1-deficient cells do not show a defect in the transbilayer phospholipid movement, which contradicts this idea.[22] Another group of proteins (called the PLSCRs for "phospholipid scramblase") has been suggested to provide the phospholipid scramblase function.[23] However, a knock-out mutation in PLSCR1 does not cause a defect in the

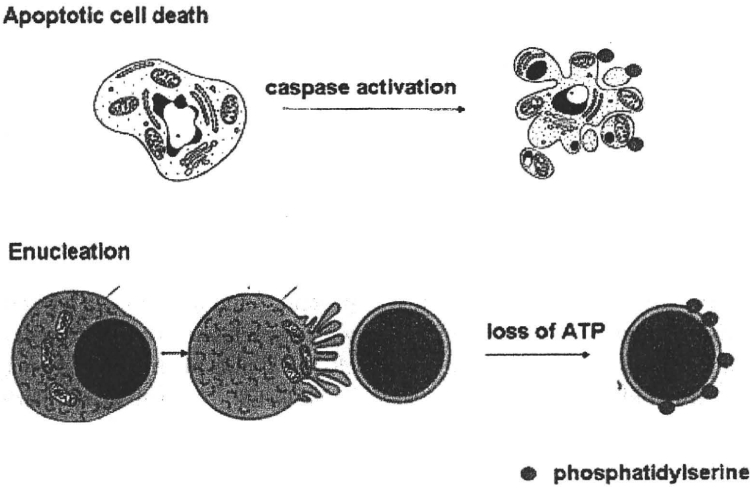

Figure 1. Exposure of phosphatidylserine on apoptotic cells and on the surface of the nuclei expelled from the erythroid precursors. Upper panel: In the apoptotic cell death process, a caspase cascade is activated via the intrinsic or extrinsic pathway. Phosphatidylserine, which works as an "eat me" signal to phagocytes, is exposed in the downstream of the caspase cascade. Lower panel: The nuclei are expelled at the final stage of definitive erythropoiesis. Owing to the lack of mitochondria and cytosol, the nuclei quickly lose ATP, leading to the inactivation of the ATP-dependent Ca pump and an increase of intracellular Ca. This would cause the inactivation of the ATP-dependent phospholipid translocases and the activation of Ca-dependent phospholipid scramblase, leading to the exposure of phosphatidylserine.

phospholipid scrambling. Rather, it transduces a signal to alter gene expression in response to various cytokines.[24] It is therefore unlikely that the PLSCRs function as scramblases.[25]

"Eat me" signal

As described earlier, apoptotic cells quickly expose phosphatidylserine on their surface. Caspase inhibitors block the exposure of phosphatidylserine in Fas ligand-induced apoptosis, indicating that the cleavage of a specific caspase substrate(s) is upstream of the phosphatidylserine exposure.[26] Chelating the intracellular Ca^{2+} also inhibits the exposure of phosphatidylserine, suggesting the involvement of Ca^{2+}-dependent scramblase in this process.[27] However, given that molecular identification of floppases and scramblases remains unclear, how phosphatidylserine is exposed during apoptotic cell death is completely unknown.

Nuclei expelled from erythroblasts expose phosphatidylserine on the plasma membrane that surrounds them[16] (Fig. 1). In this case, a lack of ATP seems to be responsible for the exposure of the phosphatidylserine, which can be explained by the following model. When the nucleus, covered by the plasma membrane, is separated from its reticulocyte, it loses the mitochondria and cytosol that are required to produce ATP (by respiration and glycolysis, respectively), leading to the inactivation of the ATP-dependent translocases.[16] The loss of ATP should also inactivate the ATP-dependent Ca^{2+} pump, increasing the intracellular Ca^{2+} concentration and the activation of Ca^{2+}-dependent scramblase. Although this is a plausible model, it can only be tested once the translocases and scramblase responsible for this process have been identified.

When phosphatidylserine is masked, phagocytosis of apoptotic cells and nuclei by macrophages is blocked,[16,28] confirming that phosphatidylserine is required for macrophages to recognize apoptotic cells. On the other hand, exposure of phosphatidylserine occurs in other situations. For example, when platelets are activated, they expose phosphatidylserine to trigger blood clotting.[29] During bone and muscle development, osteoclasts and myoblasts transiently expose phosphatidylserine and then fuse.[30,31] Activated lymphocytes also transiently expose phosphatidylserine.[32,33] These findings may indicate that the "eat me" signal of apoptotic cells may include other molecules in addition to phosphatidylserine. Alternatively, nonapoptotic phosphatidylserine-exposing cells may carry

a "don't eat me" signal on their surface. Recently, studies have proposed that calreticulin is an "eat me" signal[34] while CD47 is a "don't eat me" signal.[35] Whether these molecules work as additional "eat me" or "don't eat me" signals remains to be confirmed.

Phosphatidylserine-dependent engulfment of apoptotic cells

Macrophages and immature DCs use several distinct tricks to capture apoptotic cells (Fig. 2). Tingible-body macrophages in the germinal centers of the spleen and lymph nodes engulf the activated and apoptotic B-lymphocytes generated in germinal centers. These macrophages produce a soluble protein called milk fat globule EGF factor VIII (MFG-E8) that tightly binds to phosphatidylserine on apoptotic cells and to integrin $\alpha_v\beta_3$ or $\alpha_v\beta_5$ on the macrophages, thus serving as a bridge between apoptotic cells and macrophages.[36] Thioglycollate-elicited peritoneal macrophages also produce MFG-E8 and use it for the efficient engulfment of apoptotic cells. In support of this mechanism, knocking out the MFG-E8 gene in mice reduces the ability of the tingible-body macrophages and thioglycollate-elicited peritoneal macrophages to engulf apoptotic cells.[36,37]

Resident peritoneal macrophages express a type I membrane protein called Tim-4 that functions as a phosphatidylserine receptor for the engulfment of apoptotic cells[38]: a lack of the Tim-4 gene in mice completely abrogates their ability to engulf apoptotic cells.[39,40] In addition, Tim-3, another member of the Tim family, weakly binds to phosphatidylserine and is expressed by $CD8^+$DCs in the spleen; treatment with an anti-Tim-3 neutralizing antibody inhibits their ability to engulf apoptotic cells.[41] Other studies indicate that BAI1, a member of the secretin receptor family of the seven transmembrane protein,[42] and stabillin-2, a type I membrane protein with seven fasciclin and fifteen EGF-like domains,[43] also bind phosphatidylserine on apoptotic cells.

$MFG\text{-}E8^{-/-}$ mice, particularly females in the B6/129 mixed background, produce autoantibodies such as anti-DNA, anti-nuclear (ANA), and anti-phospholipid antibodies in an age-dependent manner and suffer from a systemic lupus erythematosus (SLE)-type autoimmune disease.[36] Because the activation of B-lymphocytes by injecting foreign antigens accelerates the development of autoimmunity in $MFG\text{-}E8^{-/-}$ mice, it is likely that the activated and dead B-lymphocytes in the germinal centers are engulfed by the tingible-body macrophages in an MFG-E8–dependent manner. When apoptotic cells are not efficiently engulfed because of the lack of MFG-E8, the unengulfed cells may undergo secondary necrosis and release their cellular contents into the extracellular space (Fig. 3). These cellular materials will activate autoreactive B-cells in the germinal centers.

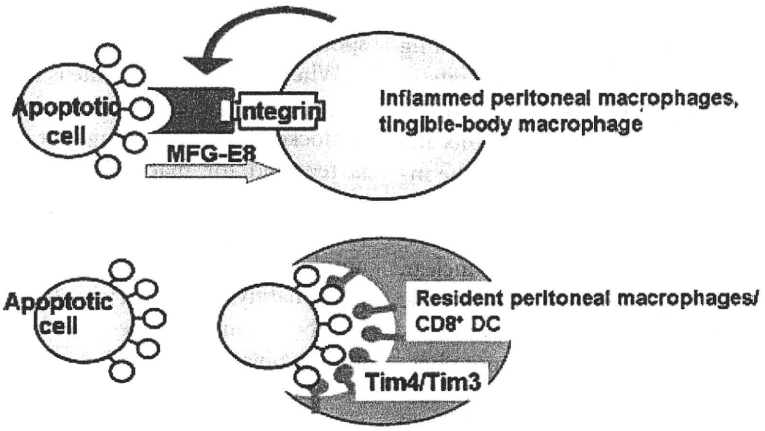

Figure 2. Distinct ways to capture apoptotic cells by different macrophages. Thioglycollate-elicited peritoneal macrophages (inflamed macrophages) and tingible-body macrophages in the spleen and lymph node secrete MFG-E8 that binds phosphatidylserine on apoptotic cells and integrin $\alpha_v\beta_3$ or integrin $\alpha_v\beta_5$ on the surface of the macrophages, thus bridging between apoptotic cells and phagocytes. Type I membrane proteins, Tim-4 and Tim-3, are expressed in resident peritoneal macrophages and $CD8^+$ dendritic cells, respectively. They bind phosphatidylserine, thus functioning as a phosphatidylserine receptor.

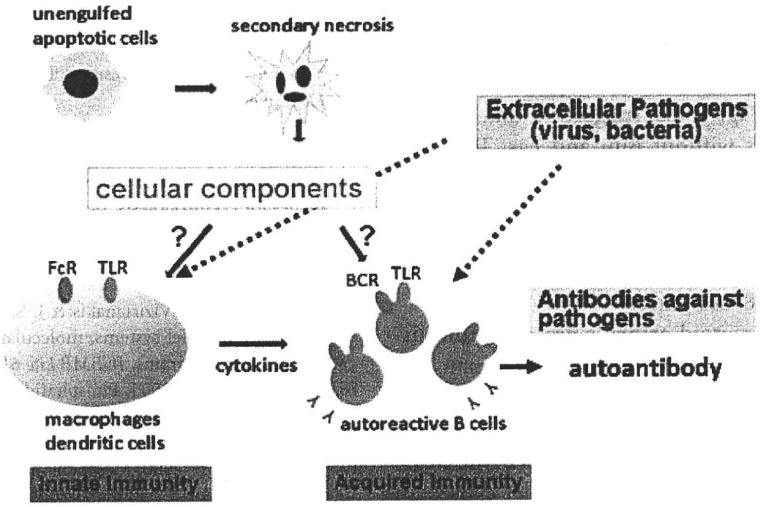

Figure 3. A model for the development of autoimmunity by dead cell's components. If apoptotic cells are not engulfed quickly, they undergo the secondary necrosis probably due to the loss of ATP, and release the cellular components. These cellular components will activate the innate immunity by binding to FcR and TLR (Toll-like receptor) on the macrophages and immature dendritic cells, while they will activate the acquired immunity by binding to BCR (B cell receptor) and TLR. This will eventually cause the production of autoantibodies against DNA, nuclei, and phospholipids. This mechanism seems to be similar to that used for the production of antibodies against extracellular pathogens.

Similarly, the administration of an anti-Tim-4 or anti-Tim-3 neutralizing antibody induces autoimmunity or the production of autoantibodies.[38,41] On the other hand, nether Tim-4- nor Tim-3-null mice produce a high level of autoantibodies.[39,40] What determines the discrepancy between the outcomes obtained by neutralization versus gene targeting is not clear. The Tim family members have multiple functions, which include regulating the T-helper type I response or the innate immune system. For example, Tim-3 modulates the function of regulatory T cells and inhibits the Th1-mediated response,[44] while Tim-4 inhibits the production of IL-2 and IFNγ by T-helper cells, which blocks T-cell proliferation.[45] Recent studies with Tim-4-deficient mice indicate that Tim-4 cell-autonomously inhibits the activation of macrophages as well.[39,40] Thus, the deficiency of Tim-3 or Tim-4 in the knockout mice may chronically inactivate the normal immune reaction that is needed for the development of autoimmunity.

Perspective

Remarkable progress has been made in understanding the molecular mechanism of apoptotic cell death and dead-cell clearance. Many molecules involved in these processes have been identified, and natural mutants and targeted mutations of these molecules have been established. Among them are mouse mutations of lymphoproliferation (*lpr*) and generalized lymphoproliferative disease (*gld*),[46] which are loss-of-function mutations of Fas and Fas ligand, respectively.[47]

Lpr and gld mice develop lymphadenopathy and splenomegaly in an age-dependent manner.[46] They produce large amounts of autoantibodies, and develop autoimmune diseases that resemble human SLE. These abnormal phenotypes of the *lpr* and *gld* mice indicate that the Fas ligand-mediated cell death plays an important role in the killing of activated autoreactive T and B cells. Activated B cells in the germinal centers of the spleen express high levels of Fas,[48] suggesting that the autoreactive B cells generated in the germinal centers may be killed by the Fas–Fas ligand system.

The production of autoantibodies in *lpr* mice is inhibited by the lack of Toll-like receptor (TLR7),[49] suggesting that the cellular components released from dead cells stimulate the immune reaction. Mice carrying mutations in both Fas and Bim develop lymphadenopathy, splenomegaly, and autoimmune disease at a much higher rate than those with a single deficiency for Fas or Bim,[50,51] indicating that both intrinsic and extrinsic death processes

operate during lymphocyte development. However, except for the abnormality in lymphocyte development, the development of other organs seems to be intact in *Bim*$^{-/-}$ *lpr* mice, suggesting that the cell death still occurs without Bim and Fas. To determine whether the cell components released from unengulfed apoptotic cells is involved in the development of autoimmune diseases in the *lpr* or *Bim*$^{-/-}$ *lpr* mice, it may be interesting to cross them with the MFG-E8-null mice.

SLE and rheumatoid arthritis are common human diseases of unknown etiology. Human patients carrying a defect in the Fas death factor develop ALPS, Autoimmune Lymphoproliferative Syndrome.[52] We now know that a defect in the clearance of dead cells and erythroid nuclei causes an SLE-type autoimmune disease or an arthritis-type autoinflammatory disease in mice.[36,53] It is time to determine whether human patients suffering from SLE or rheumatoid arthritis carry a defect in dead cell clearance in their system.[54,55]

Acknowledgments

I am grateful to all the members of my laboratory. The work in our laboratory was supported in part by grants-in-aid from the Ministry of Education, Science, Sports, and Culture in Japan.

Conflict of interest

The author declares no conflict of interest.

References

1. Danial, N.N. & S.J. Korsmeyer. 2004. Cell death: critical control points. *Cell* **116:** 205–219.
2. Vaux, D.L. & S.J. Korsmeyer. 1999. Cell death in development. *Cell* **96:** 245–254.
3. Jacobson, M.D., M. Weil & M.C. Raff. 1997. Programmed cell death in animal development. *Cell* **88:** 347–354.
4. Kerr, J.F., A.H. Wyllie & A.R. Currie. 1972. Apoptosis: a basic biological phenomenon with wide-ranging implications in tissue kinetics. *Br. J. Cancer* **26:** 239–257.
5. Nagata, S., R. Hanayama & K. Kawane. 2010. Autoimmunity and the clearance of dead cells. *Cell* **140:** 619–630.
6. Eguchi, Y., S. Shimizu & Y. Tsujimoto. 1997. Intracellular ATP levels determine cell death fate by apoptosis or necrosis. *Cancer Res.* **57:** 1835–1840.
7. Skulachev, V. 2006. Bioenergetic aspects of apoptosis, necrosis and mitoptosis. *Apoptosis* **11:** 473–485.
8. Youle, R. & A. Strasser. 2008. The BCL-2 protein family: opposing activities that mediate cell death. *Nat. Rev. Mol. Cell Biol.* **9:** 47–59.
9. Nagata, S. 1997. Apoptosis by death factor. *Cell* **88:** 355–365.
10. Luthi, A.U. & S.J. Martin. 2007. The CASBAH: a searchable database of caspase substrates. *Cell Death Differ.* **14:** 641–650.
11. Timmer, J.C. & G.S. Salvesen. 2007. Caspase substrates. *Cell Death Differ.* **14:** 66–72.
12. Palis, J. & G.B. Segel. 1998. Developmental biology of erythropoiesis. *Blood Rev.* **12:** 106–114.
13. Chasis, J.A. & N. Mohandas. 2008. Erythroblastic islands: niches for erythropoiesis. *Blood* **112:** 470–478.
14. Chasis, J.A. 2006. Erythroblastic islands: specialized microenvironmental niches for erythropoiesis. *Curr. Opin. Hematol.* **13:** 137–141.
15. Tsiftsoglou, A., I. Vizirianakis & J. Strouboulis. 2009. Erythropoiesis: model systems, molecular regulators, and developmental programs. *IUBMB Life* **61:** 800–830.
16. Yoshida, H. *et al.* 2005. Phosphatidylserine-dependent engulfment by macrophages of nuclei from erythroid precursor cells. *Nature* **437:** 754–758.
17. Wood, W. *et al.* 2000. Mesenchymal cells engulf and clear apoptotic footplate cells in macrophageless PU.1 null mouse embryos. *Development* **127:** 5245–5252.
18. Savill, J. *et al.* 2002. A blast from the past: clearance of apoptotic cells regulates immune responses. *Nat. Rev. Immunol.* **2:** 965–975.
19. Gardai, S.J. *et al.* 2006. Recognition ligands on apoptotic cells: a perspective. *J. Leuk. Biol.* **79:** 896–903.
20. Leventis, P.A. & S. Grinstein. 2010. The distribution and function of phosphatidylserine in cellular membranes. *Annu. Rev. Biophys.* **39:** 407–427.
21. Puts, C.F. & J.C. Holthuis. 2009. Mechanism and significance of P4 ATPase-catalyzed lipid transport: lessons from a Na+/K+-pump. *Biochim. Biophys. Acta.* **1791:** 603–611.
22. Williamson, P. *et al.* 2007. Transbilayer phospholipid movements in ABCA1-deficient cells. *PLoS ONE* **2:** e729.
23. Zhou, Q. *et al.* 1997. Molecular cloning of human plasma membrane phospholipid scramblase. A protein mediating transbilayer movement of plasma membrane phospholipids. *J. Biol. Chem.* **272:** 18240–18244.
24. Zhou, Q. *et al.* 2002. Normal hemostasis but defective hematopoietic response to growth factors in mice deficient in phospholipid scramblase 1. *Blood.* **99:** 4030–4038.
25. Sahu, S. *et al.* 2007. Phospholipid scramblases: an overview. *Arch. Biochem. Biophys.* **462:** 103–114.
26. Martin, S.J. *et al.* 1996. Phosphatidylserine externalization during CD95-induced apoptosis of cells and cytoplasts requires ICE/CED-3 protease activity. *J. Biol. Chem.* **271:** 28753–28756.
27. Hampton, M. *et al.* 1996. Involvement of extracellular calcium in phosphatidylserine exposure during apoptosis. *FEBS Lett.* **399:** 277–282.
28. Hanayama, R. *et al.* 2002. Identification of a factor that links apoptotic cells to phagocytes. *Nature* **417:** 182–187.
29. Lentz, B. 2003. Exposure of platelet membrane phosphatidylserine regulates blood coagulation. *Prog. Lipid Res.* **42:** 423–438.
30. Van Den Eijnde, S *et al.* 2001. Transient expression of phosphatidylserine at cell-cell contact areas is required for myotube formation. *J. Cell Sci.* **114:** 3631–3642.
31. Helming, L. & S. Gordon. 2009. Molecular mediators of macrophage fusion. *Trends Cell Biol.* **19:** 514–522.

32. Fischer, K. *et al.* 2006. Antigen recognition induces phosphatidylserine exposure on the cell surface of human CD8+ T cells. *Blood* **108:** 4094–4101.
33. Dillon, S.R. *et al.* 2000. Annexin V binds to viable B cells and colocalizes with a marker of lipid rafts upon B cell receptor activation. *J. Immunol.* **164:** 1322–1332.
34. Gardai, S.J. *et al.* 2005. Cell-surface calreticulin initiates clearance of viable or apoptotic cells through transactivation of LRP on the phagocyte. *Cell* **123:** 321–334.
35. Oldenborg, P.A. *et al.* 2000. Role of CD47 as a marker of self on red blood cells. *Science* **288:** 2051–2054.
36. Hanayama, R. *et al.* 2004. Autoimmune disease and impaired uptake of apoptotic cells in MFG-E8-deficient mice. *Science* **304:** 1147–1150.
37. Miyasaka, K. *et al.* 2004. Expression of milk fat globule epidermal growth factor 8 in immature dendritic cells for engulfment of apoptotic cells. *Eur. J. Immunol.* **34:** 1414–1422.
38. Miyanishi, M. *et al.* 2007. Identification of Tim4 as a phosphatidylserine receptor. *Nature* **450:** 435–439.
39. Rodriguez-Manzanet, R. *et al.* 2010. T and B cell hyperactivity and autoimmunity associated with niche-specific defects in apoptotic body clearance in TIM-4-deficient mice. *Proc. Natl. Acad. Sci. USA* **107:** 8706–8711.
40. Wong, K. *et al.* 2010. Phosphatidylserine receptor Tim-4 is essential for the maintenance of the homeostatic state of resident peritoneal macrophages. *Proc. Natl. Acad. Sci. USA* **107:** 8712–8717.
41. Nakayama, M. *et al.* 2009. Tim-3 mediates phagocytosis of apoptotic cells and cross-presentation. *Blood* **113:** 3821–3830.
42. Park, D. *et al.* 2007. BAI1 is an engulfment receptor for apoptotic cells upstream of the ELMO/Dock180/Rac module. *Nature* **450:** 430–434.
43. Park, S.Y. *et al.* 2008. Rapid cell corpse clearance by stabilin-2, a membrane phosphatidylserine receptor. *Cell Death Differ.* **15:** 192–201.
44. Kane, L. 2010. T cell Ig and mucin domain proteins and immunity. *J. Immunol.* **184:** 2743–2749.
45. Meyers, J.H. *et al.* 2005. TIM-4 is the ligand for TIM-1, and the TIM-1-TIM-4 interaction regulates T cell proliferation. *Nat. Immunol.* **6:** 455–464.
46. Cohen, P. & R. Eisenberg. 1991. Lpr and gld: single gene models of systemic autoimmunity and lymphoproliferative disease. *Annu. Rev. Immunol.* **9:** 243–269.
47. Nagata, S. & P. Golstein. 1995. The Fas death factor. *Science* **267:** 1449–1456.
48. Hao, Z. *et al.* 2008. Fas receptor expression in germinal-center B cells is essential for T and B lymphocyte homeostasis. *Immunity* **29:** 615–627.
49. Nickerson, K.M. *et al.* 2010. TLR9 regulates TLR7- and MyD88-dependent autoantibody production and disease in a murine model of lupus. *J. Immunol.* **184:** 1840–1848.
50. Hughes, P.D. *et al.* 2008. Apoptosis regulators Fas and Bim cooperate in shutdown of chronic immune responses and prevention of autoimmunity. *Immunity* **28:** 197–205.
51. Hutcheson, J. *et al.* 2008. Combined deficiency of proapoptotic regulators Bim and Fas results in the early onset of systemic autoimmunity. *Immunity* **28:** 206–217.
52. Holzelova, E. *et al.* 2004. Autoimmune lymphoproliferative syndrome with somatic Fas mutations. *N. Engl. J. Med.* **351:** 1409–1418.
53. Kawane, K. *et al.* 2006. Chronic polyarthritis caused by mammalian DNA that escapes from degradation in macrophages. *Nature* **443:** 998–1002.
54. Yamaguchi, H. *et al.* 2008. Milk fat globule EGF factor 8 in the serum of human patients of systemic lupus erythematosus. *J. Leuk. Biol.* **83:** 1300–1307.
55. Yamaguchi, H. *et al.* Aberrant splicing of the milk fat globule-EGF factor 8 (MFG-E8) gene in human systemic lupus erythematosus. *Eur. J. Immunol.* **40:** 1778–1785.

 DOI 10.1002/eji.201040604 Eur. J. Immunol. 2010. 40: 2590–2598

Interferon-induced TRAIL-independent cell death in *DNase II*$^{-/-}$ embryos

Yusuke Kitahara[1,2], *Kohki Kawane*[1] *and Shigekazu Nagata*[1,3]

[1] Department of Medical Chemistry, Kyoto University Graduate School of Medicine, Yoshida-Konoe, Kyoto, Japan
[2] Osaka University Medical School, Osaka, Japan
[3] Core Research for Evolutional Science and Technology, Japan Science and Technology Corporation, Yoshida-Konoe, Kyoto, Japan

The chromosomal DNA of apoptotic cells and the nuclear DNA expelled from erythroid precursors is cleaved by DNase II in lysosomes after the cells or nuclei are engulfed by macrophages. *DNase II*$^{-/-}$ embryos suffer from lethal anemia due to IFN-β produced in the macrophages carrying undigested DNA. Here, we show that Type I IFN induced a caspase-dependent cell death in human epithelial cells that were transformed to express a high level of IFN type I receptor. During this death process, a set of genes was strongly activated, one of which encoded TRAIL, a death ligand. A high level of TRAIL mRNA was also found in the fetal liver of the lethally anemic *DNase II*$^{-/-}$ embryos, and a lack of IFN type I receptor in the *DNase II*$^{-/-}$ *IFN-IR*$^{-/-}$ embryos blocked the expression of TRAIL mRNA. However, a null mutation in *TRAIL* did not rescue the lethal anemia of the *DNase II*$^{-/-}$ embryos, indicating that TRAIL is dispensable for inducing the apoptosis of erythroid cells in *DNase II*$^{-/-}$ embryos, and therefore, that there is a TRAIL-independent mechanism for the IFN-induced apoptosis.

Key words: Apoptosis · Gene expression · IFN · TRAIL

See accompanying Commentary by Crow

Introduction

Many unnecessary or potentially harmful cells are produced during animal development, and they are programmed to die by apoptosis [1, 2]. Apoptosis is morphologically characterized by the shrinkage and fragmentation of cells and their nuclei, and biochemically by DNA degradation [3]. The DNA degradation in apoptotic cells proceeds in two steps. First, the chromosomal DNA is cleaved into nucleosomal units by caspase-activated DNase in dying cells [4]. The dying cells are then engulfed by phagocytes, and their DNA is digested into nucleotides by DNase II in the lysosomes of the phagocytes [5]. During definitive erythropoiesis in the fetal liver and bone marrow, nuclei are expelled from erythroid precursor cells, and are engulfed by macrophages in the center of erythroblastic islands [6]. DNase II, expressed by the macrophages of the erythroblastic islands, is responsible for degrading the DNA of these nuclei, as well [7].

DNase II$^{-/-}$ embryos die *in utero* due to severe anemia [7]. Many fetal tissues carry accumulations of abnormal macrophages that contain undigested nuclei in their lysosomes [7]. The *IFNβ* gene is strongly activated in the tissues carrying the abnormal macrophages, and a null mutation of the IFN type I receptor gene rescues the lethality of the *DNase II*$^{-/-}$ genotype [8]. Many erythroblasts in the fetal liver of *DNase II*$^{-/-}$ embryos undergo apoptotic cell death, which is blocked by the mutation in the IFN type I receptor. These results indicate that when macrophages

Correspondence: Prof. Shigekazu Nagata
e-mail: snagata@mfour.med.kyoto-u.ac.jp

cannot digest the DNA of engulfed apoptotic cells and nuclei, they are activated to produce IFN-β, and the IFN-β causes the apoptotic cell death of erythroblasts, leading to lethal anemia in the embryos.

Type I IFN, a class of IFN cytokines that includes IFN-α and IFN-β, has an anti-viral effect [9]. It is cytotoxic for variety of cancer cells, including multiple myeloma, hairy cell leukemia, and chronic myeloid leukemia cells [10–12]. In various systems, TRAIL, a death ligand, has been proposed to mediate the apoptosis of Type I IFN-induced cell death [13–15], but many of the details underlying the cell death remain obscure.

Here, we examine the mechanism underlying the Type I IFN-induced cell death. We show that the treatment of human FL cells with Type I IFN rendered the cells resistant to virus, but it did not kill them. On the other hand, FL cells exogenously overexpressing the IFN type I receptor were killed by IFN-α in a caspase-dependent manner. This cell death process was accompanied by the induction of a specific set of genes, which was not observed when the parental FL cells were treated with IFN-α. An overlapping but different set of genes was activated in the fetal liver of *DNase II*$^{-/-}$ embryos, in which erythroblasts undergo apoptotic cell death in a Type I IFN-dependent manner. One of the genes that was activated in both the IFN-α-treated human FL cells overexpressing IFN receptor and the *DNase II*$^{-/-}$ mouse fetal liver was TRAIL. However, a null mutation of *TRAIL* did not rescue the lethality of *DNase II*$^{-/-}$ embryos, suggesting that TRAIL is dispensable for the IFN-induced cell death, at least in the *DNase II*$^{-/-}$ embryos.

Results

IFN-α-induced apoptosis

The receptor for Type I IFN consists of two subunits, R1 and R2 [16]. Human FL cells intrinsically express both R1 and R2, and the treatment of FL cells with IFN-α2 rendered them resistant to Mengo virus in a dose-dependent manner (Fig. 1A and B). On the other hand, the treatment of FL cells with 10 000 units of IFN-α2 did not inhibit their growth (Fig. 1C). The effect of a cytokine can often be potentiated by the increased availability of its receptor. To increase the sensitivity of the FL cells to IFN-α, the cDNA for the R1 and R2 subunits of the IFN type-I receptor were introduced into FL cells, and FL transformant lines expressing either R1 (FR1) or R2 (FR2), or both (F19 and F27) were established (Fig. 1A).

As shown in Fig. 1B, overexpression of the R1 and R2 subunits in the FL cell transformants did not significantly change the cells' sensitivity to the anti-viral activity of IFN-α2. On the other hand, the overexpression of the IFN receptor rendered the FL cells sensitive to the cytotoxic activity of IFN-α2. More than 50% of the F19 cells, which expressed both the R1 and the R2 subunits, were killed within 48 h by 10 000 units/mL of IFN-α. On the contrary, the expression of either the Rl or the R2 IFN receptor subunit alone did not increase the sensitivity of the FL cells to IFN-α

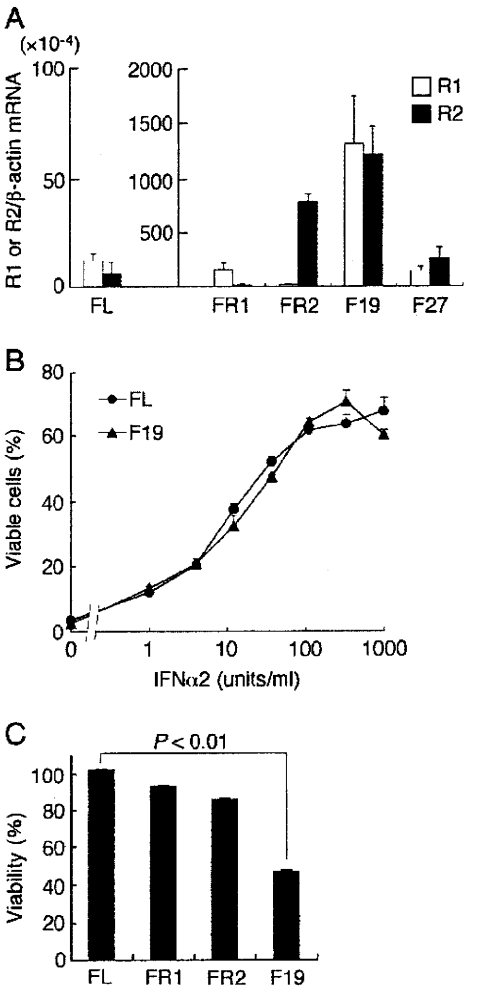

Figure 1. Establishment of FL cell transformants overexpressing the IFN type I receptor. An expression plasmid for the R1 or R2 subunit of the human IFN type I receptor was introduced into human FL cells, and transformants expressing the R1 subunit (FR1) or R2 subunit (FR2) alone, or both the R1 and the R2 subunits (F19 and F27) were established. (A) The mRNA levels of the R1 (open bars) and R2 (closed bars) subunits in the parental FL, FR1, FR2, F19, and F27 transformants were determined by RT-PCR. They are expressed as a value relative to the β-actin mRNA level. The RT-PCR was performed in triplicate, and average values are shown with SD. (B) Human FL cells (closed circles) and F19 cells (closed triangles) were treated with the indicated concentrations of recombinant human IFN-α2 for 6 h, and challenged with Mengo virus for 24 h. The viable cells were then stained with crystal violet, and are shown as a percentage of the cells without virus treatment. The experiment was performed in triplicate, and the average values are shown with SD. (C) The parental FL cells, and the FR1, FR2, and F19 cells were treated with 10 000 units/mL of human IFN-α2 for 48 h, and their viability was determined by FACS analysis after staining with Annexin V and PI. The viability of the IFN-treated cells is expressed as a percentage of that of cells incubated without IFN. The experiments were performed three times, and the average values are shown with SD. The *p*-value, determined by Student's t-test is shown.

(Fig. 1C). A higher dose of IFN-α2 was needed to elicit its cytotoxic activity than its anti-viral activity. That is, 1000 units of IFN-α2 was sufficient for the maximum anti-viral activity in FL and

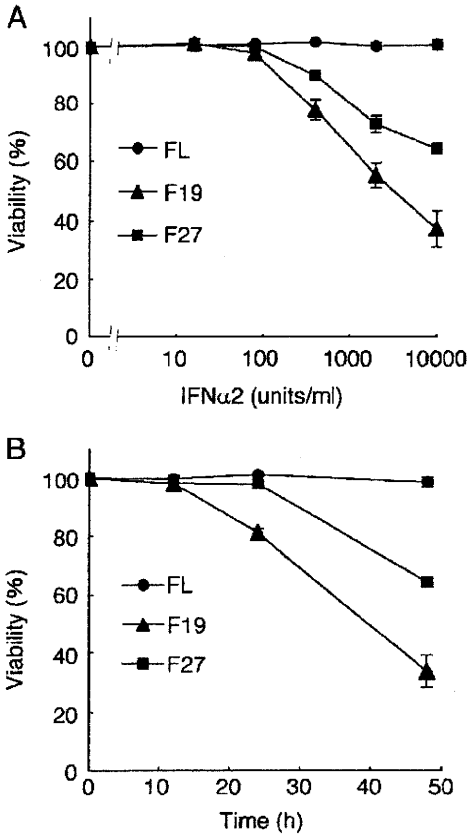

Figure 2. The cell death induced by IFN-α2. The parental FL cells (closed circles) and the FL cell transformants expressing the IFN type I receptor, F19 (closed triangles) and F27 (closed squares), were treated with the indicated concentrations of human IFN-α2 for 48 h (A) or with 10 000 units/mL of human IFN-α2 for the indicated periods of time (B). After the incubation, the cells were stained with Annexin V and PI, and their viability was determined by FACS. The viability of the IFN-treated cells is expressed as a percentage of that of cells incubated without IFN. The experiments were performed in triplicate, and the average values are shown with SD.

F19 cells (Fig. 1B), whereas 10 000 units of IFN-α2 were required to kill about 70% of the F19 cells (Fig. 2A). In addition, a 6-h incubation was sufficient to detect IFN-α2's anti-viral activity, whereas it took more than 48 h to kill F19 cells with IFN-α2 (Fig. 2B). The susceptibility to IFN-α's cytotoxic activity was more prominent with F19 cells than F27 cells. This is probably because the expression level of R1 and R2 subunits is 8.3 and 4.6 times higher in F19 cells than F27 cells (Fig. 1A).

Caspase-dependent cell death induced by IFN-α2

The FL cells as well as their F19 and F27 transformants could be killed by Fas ligand, and this cell death process was inhibited by treatment with 100 μM z-VAD, a pan-caspase inhibitor (Fig. 3A and data not shown). An analysis by Western blotting showed that the treatment of FL cells with Fas ligand caused the processing of pro-caspase 3 into the p20 and p19 fragments

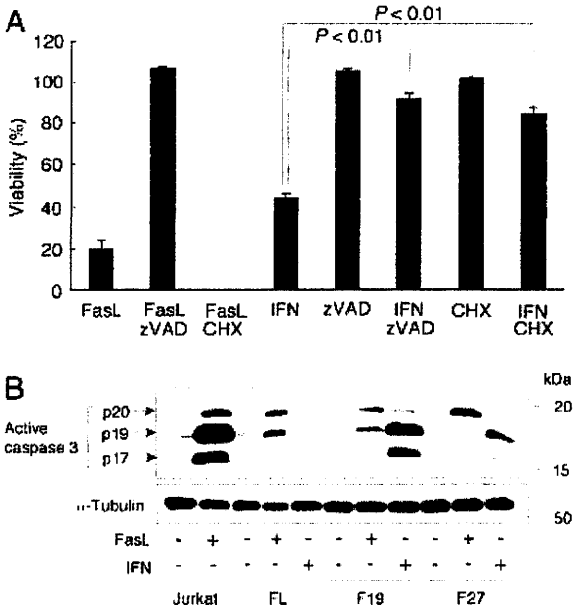

Figure 3. Caspase-mediated cell death by IFN-α2. (A) Effect of caspase inhibitor on the IFN-α2-induced cell death. After preincubation with or without 100 μM z-VAD-fmk or 2.5 μM cycloheximide for 1 h, F19 cells were incubated with 10 000 units/mL IFN-α2 for 48 h, and the percentage of viable cells (Annexin V$^-$ and PI$^-$) was determined. As a control, F19 cells were treated with Fas ligand in the presence or absence of z-VAD-fmk or cycloheximide. zVAD, z-VAD-fmk; IFN, IFN-α2; FasL, Fas ligand; CHX, cycloheximide. The experiments were performed three times, and the average values are plotted with SD. The *p*-values, determined by Student's *t*-test, are shown. (B) Activation of caspase 3 by IFN-α2. FL, F19, and F27 cells were treated with 10 000 units/mL IFN-α2 for 48 h, and the cell lysates were analyzed by Western blotting with rabbit Ab against active caspase 3. As a loading control, the same membrane was blotted with an Ab against α-tubulin. Human Jurkat cells were treated with Fas ligand for 2 h, and the cell lysate was used as the positive control for active caspase 3.

representing its active form. The IFN-α-induced cell death in F19 and F27 cells was also blocked by the treatment of the cells with 100 μM z-VAD (Fig. 3), and the p19 and p17 fragments of active caspase 3 were observed in the cell lysates from IFN-α-treated F19 and F27 but not FL cells. These results indicated that IFN-α induced caspase-dependent apoptosis in F19 and F27 cells, which expressed a high level of the IFN receptor.

Gene expression in FL cell transformants over-expressing the IFN receptor

Fas ligand killed the FL cells within 2–3 h. In this rapid, Fas ligand-induced cell death, caspases are directly activated *via* the Fas death receptor with no involvement of newly synthesized gene products [17]. On the other hand, the IFN-α2-induced death of the F19 and F27 cells took more than 40 h, even with a saturating concentration of IFN-α2. Cycloheximide, an inhibitor of protein synthesis that enhances the Fas ligand-induced apoptosis, inhibited the IFN-α-induced cell death (Fig. 3A). This result suggested that the IFN-α-induced cell death requires newly

synthesized gene products, the expression of which is induced by IFN-α. To examine the possible IFN-α-target genes responsible for the cell killing, we compared the gene expression profiles of the IFN-α2-treated FL and F19 cells by microarray analysis.

As summarized in Table 1, the expression of a set of genes including *Xaf1* (XIAP-associated factor 1), *Oas* (2′-5′-oligoadenylate synthetase), and *MX2* (myxovirus resistance 2) was upregulated by IFN-α2 in FL as well as F19 cells. These genes were activated 30- to 1300-fold by IFN-α2, and the difference in the induction between the FL and the F19 cells was threefold at most. The genes that were upregulated in FL cells by IFN-α2 were also upregulated in the fetal liver of *DNase II*$^{-/-}$ embryos. The expression of these genes in *DNase II*$^{-/-}$ embryos was drastically reduced by the lack of the IFN type I receptor (Table 1), indicating that most of the genes in this category were activated by Type I IFN in human FL cells and *DNase II*$^{-/-}$ fetal liver.

In F19 cells, another set of genes was strongly and specifically upregulated (Table 2). For example, expression of the *Indo* (indoleamine-pyrrole 2,3 dioxygenase) gene was upregulated 36 times in FL cells by IFN-α2, but its expression level increased more than 20 000-fold by the treatment with IFN-α2 in F19 cells. The *CXCL10* and *CXCL11* genes were upregulated by IFN-α2 less than tenfold in FL cells, but more than 10 000-fold in F19 cells. Among the death ligands (TRAIL, TNFα, and Fas ligand), TRAIL was in this group. That is, the TRAIL mRNA level increased 2800-fold in F19 cells after IFN-α2 treatment, but 35-fold in FL cells. The TNF mRNA level also increased in IFN-α2-treated F19 cells, but the increase was only eightfold (data not shown). The Fas ligand gene was not activated by IFN-α in either the FL or the F19 cells.

IFN-dependent expression of TRAIL in FL cells and *DNase II*$^{-/-}$ mouse embryos

The time course of the gene induction, assayed by real-time PCR, indicated that the TRAIL mRNA in F19 cells started to increase at 6 h after the stimulation with IFN-α2, and reached its maximum level (1500-fold compared with the level before treatment) at 24 h (Fig. 4A). The TRAIL mRNA level then declined, probably due to the cell death caused by IFN-α2. In contrast to TRAIL, the levels of the Fas ligand and TNFα mRNAs were not affected by the IFN-α treatment in F19 cells.

In *DNase II*$^{-/-}$ embryos, erythroblasts in the fetal liver undergo apoptosis, and the embryos die due to severe anemia. This *DNase II*$^{-/-}$-induced embryonic lethality can be rescued by a null-mutation in the *IFN type I receptor* gene, indicating that genes induced *via* Type I IFN in the *DNase II*$^{-/-}$ embryos are responsible for killing the embryos [8]. As summarized in Table 2, among the genes that were exclusively upregulated in the IFN-α2-treated F19 cells, only a few were upregulated in the *DNase II*$^{-/-}$ fetal liver in an IFN-dependent manner. The TRAIL gene was one of them. That is, the TRAIL mRNA level was 30- to 60-fold higher in the

Table 1. Genes upregulated by Type I IFN in human FL and F19 cells[a]

Symbol (gene title)	Human cells						Mouse fetal liver				
	FL			F19			WT	DNase II$^{-/-}$		DNase II$^{-/-}$ IFN-IR$^{-/-}$	
	Signal			Signal							
	0 h	24 h	Fold	0 h	24 h	Fold	Signal	Signal	Fold	Signal	Fold
Xaf1 (XIAP-associated factor 1)	5.8	7491.1	1291.6	18.3	23 246.9	1270.3	167.2	7523.1	45.0	71.1	0.4
Trim22 (tripartite motif-containing 22)	5.0	2989.3	597.9	14.6	12 031.6	824.1					
Ifitm1 (IFN-induced transmembrane protein 1)	186.0	57 114.6	307.1	875.5	110 578.2	126.3	769.3	4113.1	5.3	1583.8	2.1
Oas2 (2′-5′-oligoadenylate synthetase 2)	5.1	1380.8	270.7	12.4	2761.6	222.7	131.8	3293.5	25.0	84.6	0.6
Ifi6 (IFN, α-inducible protein 6)	186.1	27 834.4	149.6	614.2	38 877.6	63.3					
MX2 (myxovirus (influenza virus) resistance 2)	13.4	1791.7	133.7	12.7	3746.9	295.0	7.6	372.1	49.0	6.2	0.8
Hsh2d (hematopoietic SH2 domain containing)	28.1	2851.6	101.5	66.5	6852.1	103.0	18.8	416.5	22.2	3.1	0.2
Lamp3 (lysosomal-associated membrane protein 3)	80.1	7711.6	96.3	133.6	30 017.2	224.7					
Ifi44 (IFN-induced protein 44)	298.9	22 560.5	75.5	1223.7	38 144.8	31.2	59.8	2062.8	34.5	5.1	0.1
Oas1 (2′-5′-oligoadenylate synthetase1)	410.6	16 095.8	39.2	842.3	32 352.8	38.4	369.5	10 121.7	27.4	105.6	0.3

[a] Human FL and F19 cells were stimulated with IFN-α2 for 24 h, and their RNA were analyzed by microarray as described in *Materials and methods*. The induction (fold) was calculated by dividing the signal at 24 h by the signal at 0 h, and the ten genes that most strongly activated by IFN-α2 in FL cells are listed. The expression of the corresponding genes in the WT, *DNase II*$^{-/-}$, and *DNase II*$^{-/-}$*IFN-IR*$^{-/-}$ mouse fetal livers [8] is shown in the table at right. The signals in the *DNase II*$^{-/-}$ and *DNase II*$^{-/-}$*IFN-IR*$^{-/-}$ fetal liver were divided by the signal in the WT fetal liver, and are shown as "Fold".

Table 2. Genes upregulated by Type I IFN specifically in F19 cells[a)]

Symbol (gene title)	Human Cells									Mouse fetal liver				
	FL			F19			Specific induction[a)]	p-Value[a)]	pFDR[a)]					
	Signal			Signal						WT	DNase $II^{-/-}$		DNase $II^{-/-}$ $IFN\text{-}IR^{-/-}$	
	0 h	24 h	24/0 h Fold	0 h	24 h	24/0 h Fold				Signal	Signal	Fold	Signal	Fold
Cxcl10 (chemokine (C-X-C motif) ligand 10)	2.7	15.6	5.8	2.5	49834.2	19933.7	3436.8	0.0	0.0	397.1	7855.9	19.8	3242.6	8.2
Cxcl11 (chemokine (C-X-C motif) ligand 11)	6.7	53.0	7.9	3.0	40572.0	13524.0	1711.9	0.0	0.0	1.9	35.1	18.5	5.6	2.9
Gbp4 (guanylate-binding protein 4)	2.5	5.8	2.3	2.3	3694.7	1606.4	698.4	0.0	0.0	125.2	1579.3	12.6	201.8	1.6
Indo (indoleamine-pyrrole 2,3 dioxygenase)	8.0	290.6	36.3	3.3	70983.1	21510.0	592.6	0.0	0.0	49.7	46.0	0.9	41.9	0.8
C6orf32 (chr. 6 open reading frame 32)	2.6	4.2	1.6	2.4	1696.7	707.0	441.9	0.0	0.0	181.6	270.0	1.5	230.4	1.3
Bcl2l14 (BCL2-like 14)	2.4	4.5	1.9	2.3	628.9	273.4	143.9	2.1×10^{-13}	9.3×10^{-10}	41.7	53.0	1.3	30.9	0.7
Tgm2 (transglutaminase 2)	68.9	110.0	1.6	15.7	2435.9	155.2	97.0	1.6×10^{-11}	4.3×10^{-8}	3106.2	4583.8	1.5	4006.9	1.3
Trail (TNF-related apoptosis-inducing ligand)	11.8	422.8	35.8	8.8	24699.3	2806.7	78.4	1.2×10^{-10}	2.4×10^{-7}	2.7	138.9	51.4	3.1	1.1
Sept4 (septin 4)	11.0	4.2	0.4	6.8	173.2	25.5	63.8	5.4×10^{-10}	8.2×10^{-7}	385.6	411.3	1.1	442.6	1.1
Hippi (HIP1 protein interactor)	8.7	11.0	1.3	2.4	107.9	45.0	34.6	1.3×10^{-7}	7.5×10^{-5}	172.8	373.9	2.2	278.8	1.6
Ubd (ubiquitin D)	16.3	26.6	1.6	22.1	981.1	44.4	27.8	8.1×10^{-7}	3.8×10^{-4}	62.6	39.1	0.6	76.0	1.2

[a)] Human FL and F19 cells were stimulated with IFN-α2 for 24 h, and their RNA were analyzed by microarray as described in *Materials and methods*. The induction (fold) was calculated by dividing the signal at 24 h by the signal at 0 h, and the 11 genes that were most strongly activated by IFN-α2 in the F19 cells are listed. To show the enhanced induction in F19 cells by IFN-α2, the induction fold obtained with F19 cells was divided by one obtained with FL cells, and shown as "Specific induction". The data were analyzed statistically with false discovery rate method using R-software, and the obtained *p*-values and pFDR values are shown. The expression of the corresponding genes in the WT, *DNase* $II^{-/-}$, and *DNase* $II^{-/-}$ $IFN\text{-}IR^{-/-}$ mouse fetal livers [8] is shown in the table at right. The signals in the *DNase* $II^{-/-}$ and *DNase* $II^{-/-}$ $IFN\text{-}IR^{-/-}$ fetal liver were divided by the signal in the WT fetal liver, and are shown as "Fold".

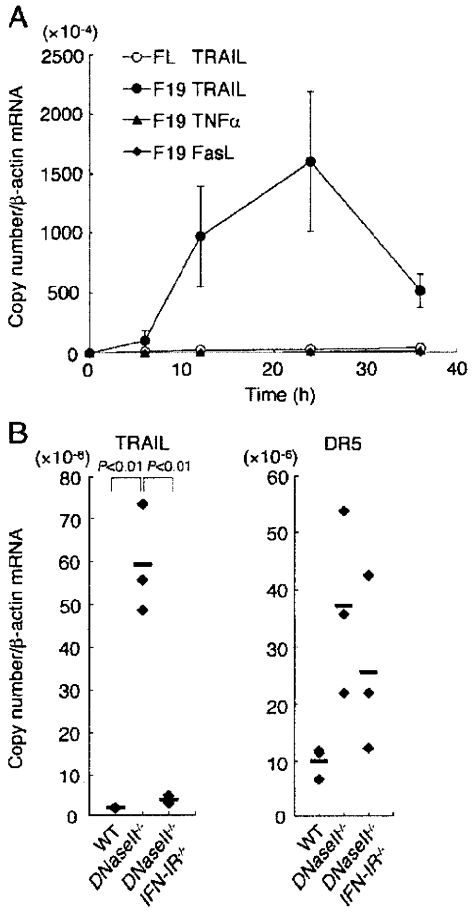

Figure 4. Induction of TRAIL gene expression by IFN-α2. (A) IFN-α2 induced the expression of TRAIL in F19 cells. FL and F19 cells were incubated with 10000 units/mL of human IFN-α2 for the indicated periods of time, and then their total RNA was prepared. The mRNA levels for Fas ligand, TNFα, and TRAIL were quantified by real-time PCR and are expressed relative to the β-actin mRNA level. The RT-PCR was carried out in triplicate, and the average values were plotted. (B) IFN-dependent expression of TRAIL in the fetal liver of *DNase II*$^{-/-}$ mice. RNA was prepared from WT, *DNase II*$^{-/-}$, and *DNase II*$^{-/-}$*IFN-IR*$^{-/-}$ fetal livers at E14.5 (three mice for each genotype). The mRNA levels of TRAIL and DR5 were quantified by real-time PCR, and are expressed as a value relative to the β-actin mRNA level. The value obtained by each mouse is plotted with an average value (bars). The *p*-values, determined by Student's *t*-test, are shown.

Table 3. No effect of TRAIL-null mutation on the lethality of DNase II$^{-/-}$ embryos[a)]

Genotype	DNase II$^{+/+}$	DNase II$^{+/-}$	DNase II$^{-/-}$
+/+	21	35	0
IFN-IR$^{-/-}$	19	36	23
TRAIL$^{-/-}$	17	24	0

[a)] Mice carrying the *DNase II*$^{+/-}$, *DNase II*$^{+/-}$*IFN-IR*$^{-/-}$, and *DNase II*$^{+/-}$*TRAIL*$^{-/-}$ genotypes were intercrossed, and the genotype for the *DNase II* gene in their offspring was determined by PCR. The number of offspring carrying the indicated genotype is shown. Results of the intercrosses of *DNase II*$^{+/-}$, *DNase II*$^{+/-}$ *IFN-IR*$^{-/-}$ are from Yoshida *et al.* [8].

DNase II$^{-/-}$ fetal liver than that in WT embryos, and was completely returned to the control level by a null mutation of the *IFN type I receptor* gene (Table 2 and Fig. 4B).

TRAIL has cytotoxic activity, particularly for tumor cells [18–20]. It also induces apoptosis in erythroblasts, and inhibits erythropoiesis by activating the ERK signaling cascade [21]. DR5, a receptor for TRAIL, was expressed in the *DNase II*$^{-/-}$ and *DNase II*$^{-/-}$ *IFN-IR*$^{-/-}$ fetal liver (Fig. 4B). We therefore examined the involvement of TRAIL in the lethality of *DNase II*$^{-/-}$ embryos, by establishing and intercrossing *DNase II*$^{+/-}$ mice in a *TRAIL*-null background. As summarized in Table 3, no *DNase II*$^{-/-}$*TRAIL*$^{-/-}$ double mutant mice were born from seven mothers. The *DNase II*$^{-/-}$*TRAIL*$^{-/-}$ embryos were severely anemic at E15.5, and the hematocrit was comparable between the *DNase II*$^{-/-}$ and the *DNase II*$^{-/-}$*TRAIL*$^{-/-}$ embryos, indicating that TRAIL is dispensable for inducing the lethal anemia in *DNase II*$^{-/-}$ embryos.

Discussion

In this report, we established human epithelial cell lines that overexpressed the IFN type I receptor. The sensitivity of the transformants to the anti-viral activity of IFN-α2 did not change with the overexpression of the IFN receptor. On the other hand, the sensitivity to IFN-α-induced cell death dramatically increased with the receptor's overexpression. That is, the parental human FL cells were resistant to IFN-α2-induced cell death, but the transformants overexpressing the IFN receptor underwent caspase-dependent cell death upon treatment with IFN-α2. The similar effect, the enhanced susceptibility to the IFN-α-induced cell death accompanied by the TRAIL gene induction, was observed with mouse L-cells overexpressing IFN type I receptor (data not shown).

Type I IFN exerts its activity through a signal transduction pathway involving JAK and STAT proteins [22]. A complex of STAT1, STAT2, and IRF9, known as IFN-stimulated gene factor 3 (ISGF3), activates the transcription of IFN-α/β-inducible genes by binding to the IFN-stimulated response element (ISRE). The ISRE is present in the promoter region of *OAS* and *MX*, which are well-known IFN-inducible genes that may be involved in the antiviral effects of IFN [23]. The mRNA levels of *OAS* and *MX* were equally upregulated in the FL and F19 cells after IFN treatment, suggesting that the IFN-α2-induced JAK/STAT-mediated gene expression pathway is not accelerated by the overexpression of the IFN type I receptor. This result also suggests that the gene products activated by the JAK/STAT pathway alone are not sufficient to activate the cell death pathway, and agrees with the previous reports suggesting that the NF-κB, p53, and PI3K/mTOR pathways are involved in the IFN-induced cell death [24–28]. In any case, how the overexpression of the IFN receptor changed the cells' sensitivity to IFN's cytotoxicity is an interesting subject for future study. In addition, whether the different sensitivities of various tumor cells to the cytotoxicity of Type I IFN can be explained by a change in the molecular components or the strength of the downstream signaling pathway remains to be studied.

The expression of genes for death ligands such as TNFα, Fas ligand, and TRAIL induced by Type I IFN has been reported in various systems [13, 14, 29]. In particular, TRAIL was proposed to mediate the IFN-induced cytotoxicity in human myeloma, hepatoma, and bladder cancer [30–32]. We also observed strong IFN-dependent induction of the *TRAIL* gene in human FL cells expressing the IFN type I receptor, as well as in *DNase II*$^{-/-}$ mouse embryos. However, the lethal anemia caused by IFN-β produced in the *DNase II*$^{-/-}$ embryos was not rescued by null mutation of the TRAIL gene, indicating that TRAIL is dispensable for the IFN-induced cytotoxicity, at least in *DNase II*$^{-/-}$ mouse embryos. Several apoptosis-related genes (*Bcl2-like14*, *Transglutaminase 2*, *Septin 4*, *Hippi*, and *Ubiquitin D*) were strongly upregulated by IFN-α2 specifically in the cells overexpressing the IFN receptor (F19) (Table 2). Whether any of these genes alone, in combination, or together with TRAIL are responsible for the IFN-induced cell death remains to be studied.

Type I IFN are clinically useful as anti-viral agents for patients with chronic hepatitis C, and as drugs to treat cancers of various origins [9]. Although IFN treatment is beneficial for these patients, it has side effects (fatigue, fever, myalgia, and depression) when administered in high doses [33]. IFN-α is also believed to be responsible for the inflammation associated with systemic lupus erythematosus [34]. Identification of the respective genes responsible for the IFN-induced anti-viral activity, cell death, and inflammation should further increase the therapeutic potential of Type I IFN.

Materials and methods

Mice

The *DNase II*$^{-/-}$ and *DNase II*$^{-/-}$*IFN-IR*$^{-/-}$ mice were described previously [7, 8]. The *TRAIL*$^{-/-}$ mice [35] were provided by Dr. Roy Black (Amgen, USA). The mice were housed in a specific pathogen-free facility at Kyoto University Graduate School of Medicine. All animal experiments were performed in accordance with protocols approved by the Animal Care and Use Committee of Kyoto University Graduate School of Medicine.

To determine the genotype of *DNase II*$^{-/-}$, *IFN-IR*$^{-/-}$, and *TRAIL*$^{-/-}$ mice, DNA was prepared from embryonic tissue or a tail snip of adult mice as described previously [36], and analyzed by PCR. The primers for genotyping *DNase II*$^{-/-}$ and *IFN-IR*$^{-/-}$ mice have been described [8]. For the WT and mutant allele of the *TRAIL* gene, a sense primer specific for the WT (5′-ACTTCATGGCCTCCTCATGGTCAG-3′) or mutant allele (5′-GGACCGCTATCAGGACATAGCGTTG-3′; a sequence in the neomycin-resistance gene) was used with a common antisense primer (5′-GGTATGTGGGGCCTTACATGCTTC-3′).

Cells and reagents

Human FL cells (ATCC CCL-62) were cloned and cultured in DMEM containing 10% FCS. To establish FL cell transformants expressing the IFN type I receptor, the coding sequences for human *IFNAR1* (GenBank Accession number: BC021825) [37] and *IFNAR2c* (GenBank Accession number: NM_207585) [38] were inserted into pEF-BOS [39], and introduced into FL cells with a hygromycin-resistance gene (pMiw-hyg) by FuGENE6 (Roche Diagnostics, Basel, Switzerland). The hygromycin-resistant clones were selected by culturing the cells in the presence of 600 μg/mL hygromycin, and the cells expressing IFNAR1 and IFNAR2c were identified by real-time PCR.

The leucine-zipper-tagged human Fas ligand (Fas ligand) was produced by transfecting monkey COS cells with the expression vector as described previously [40]. Recombinant human IFN-α2 produced in *Escherichia coli* was provided by Dr. Charles Weissmann (Scripps Research Institute-Florida, Jupiter, FL, USA). A caspase inhibitor, z-VAD-fmk [benzyloxycarbonyl-Val-Ala-Asp (OMe) fluoromethylketone], was purchased from Peptide Institute (Osaka, Japan).

Assay for the anti-viral activity of IFN

The anti-viral activity of IFN was determined using human FL cells and Mengo virus [41]. In brief, 2×10^4 FL cells in each well of a 96-well microtiter plate were treated at 37°C for 6 h with an IFN sample, and challenged at 37°C for 24 h with Mengo virus. The living cells were stained with crystal violet. Fifty units of recombinant human IFN-α2 reduced the cytopathic effect of the virus by 50% in this assay system.

Assay for the cytotoxic activity of IFN

To determine the cytotoxic activity of IFN, 2×10^4 human FL cells in each well of a 48-microtiter plate were treated at 37°C with IFN, stained with Annexin V and PI, and analyzed by flow cytometry [8].

Real-time PCR and microarray analysis

Total RNA was prepared from human FL cells and mouse tissues using an RNeasy Mini Kit (Qiagen, Hilden, Germany) and RNase-free DNase I (Qiagen), and reverse-transcribed using Superscript III (Invitrogen, Carlsbad, CA, USA) with Oligo(dT) or random hexamer as the primer. Real-time PCR was carried out using the LightCycler system (Roche Diagnostics) with the following primers for the mouse sequences: TRAIL, 5′-TGGAGAGATCTTGAACAGACCC-3′ and 5′-AGGGAGGAGTACTTAGCTGC-3′; DR5, 5′-GTTGCTGCTTGCTGTGCTAC-3′ and 5′-GCTTGCAGTTCCCTTCTGAC-3′; and β-actin, 5′-TGTGATGGTGGGAATGGGTCAG-3′ and 5′-TTTGATGTCACGCACGATTTCC-3′; and for human sequences: Fas ligand, 5′-GCCTGTGTCTCCTTGTGATG-3′ and 5′-TCTGCCAGCTCCTTCTGTAG-3′; TNFα, 5′-GCCTGTAGCCCATGTTGTAG-3′ and 5′-GAAGAGGACCTGGGAGTAGATG-3′; TRAIL, 5′-GCAGATGCAGGACAAGTACTC-3′ and 5′-ACTTGACTTGCCAGCAGG-3′; and β-actin,

5′-GCATCCTCACCCTGAAGTAC-3′ and 5′-CTTAATGTCACGCAC-GATTTC-3′.

The microarray analysis was carried out using the Whole Human Genome Oligo Microarray kit (Agilent Technologies, Santa Clara, CA, USA). Double-stranded cDNA was prepared using the total RNA from FL cells and F19 cells (FL cells over-expressing the receptor for Type I IFN) that had been stimulated with IFN-α2 (10 000 U/mL) for 0 and 24 h, and transcribed *in vitro* with cyanine three-labeled CTP. The complementary RNA was used as a probe for hybridization of the array. The hybridized RNA was detected with an Agilent Microarray scanner, and the array image was analyzed with Feature Extraction Software and GeneSpring Software (Agilent Technologies).

Western blotting

Cells (3×10^5 cells) were lysed with 200 μL lysis buffer (50 mM Tris-HCl, pH 7.5, 150 mM NaCl, 1 mM EDTA, 1% Triton, and 1 μg/mL leupeptin), and the insoluble material was removed by centrifugation. Supernatant containing 10 μg of protein was heated at 95°C for 5 min in 1 × Sample buffer (2% SDS, 62.5 mM Tris-HCl, pH 6.8, 10% glycerol, 50 mM DTT, and 0.01% BPB), and separated by electrophoresis on a 10–20% polyacrylamide gel. The proteins were transferred to a PVDF membrane (Millipore, Bedford, MA, USA) and subjected to Western blotting with rabbit Ab against human active caspase 3 (Cell Signaling, Danvers, MA, USA) or a mouse mAb against α-tubulin (Calbiochem, San Diego, CA, USA). Proteins recognized by the primary Ab were reacted with HRP-conjugated goat anti-rabbit Ig (Dako Cytomation, Glostrup, Denmark) or anti-mouse Ig (Dako Cytomation) and visualized using ECL (PerkinElmer Life Science, Boston, MA, USA).

The authors thank Dr. Roy Black, Amgen, Department of Inflammation, Seattle, for *TRAIL*$^{-/-}$ mice, and Dr. Ryo Yamada, Center for Genomic Medicine, Kyoto University Graduate School of Medicine, for statistical analysis. The authors thank Mses. M. Fujii and M. Harayama for secretarial assistance. This work was supported in part by Grants-in-Aid from the Ministry of Education, Science, Sports, and Culture in Japan.

The authors declare no financial or commercial conflict of interest.

References

1 Jacobson, M. D., Weil, M. and Raff, M. C., Programmed cell death in animal development. *Cell* 1997. **88**: 347–354.

2 Vaux, D. L. and Korsmeyer, S. J., Cell death in development. *Cell* 1999. **96**: 245–254.

3 Wyllie, A. H., Kerr, J. F. R. and Currie, A. R., Cell death: the significance of apoptosis. *Int. Rev. Cytol.* 1980. **68**: 251–306.

4 Enari, M., Sakahira, H., Yokoyama, H., Okawa, H., Iwamatsu, A. and Nagata, S., A caspase-activated DNase that degrades DNA during apoptosis, and its inhibitor ICAD. *Nature* 1998. **391**: 43–50.

5 Kawane, K., Fukuyama, H., Yoshida, H., Nagase, H., Ohsawa, Y., Uchiyama, Y., Iida, T. *et al.*, Impaired thymic development in mouse embryos deficient in apoptotic DNA degradation. *Nat. Immunol.* 2003. **4**: 138–144.

6 Chasis, J. A. and Mohandas, N., Erythroblastic islands: niches for erythropoiesis. *Blood* 2008. **112**: 470–478.

7 Kawane, K., Fukuyama, H., Kondoh, G., Takeda, J., Ohsawa, Y., Uchiyama, Y. and Nagata, S., Requirement of DNase II for definitive erythropoiesis in the mouse fetal liver. *Science* 2001. **292**: 1546–1549.

8 Yoshida, H., Okabe, Y., Kawane, K., Fukuyama, H. and Nagata, S., Lethal anemia caused by interferon-beta produced in mouse embryos carrying undigested DNA. *Nat. Immunol.* 2005. **6**: 49–56.

9 Borden, E. C., Sen, G. C., Uze, G., Silverman, R. H., Ransohoff, R. M., Foster, G. R. and Stark, G. R., Interferons at age 50: past, current and future impact on biomedicine. *Nat. Rev. Drug Discov.* 2007. **6**: 975–990.

10 Gomez-Benito, M., Balsas, P., Carvajal-Vergara, X., Pandiella, A., Anel, A., Marzo, I. and Naval, J., Mechanism of apoptosis induced by IFN-alpha in human myeloma cells: role of Jak1 and Bim and potentiation by rapamycin. *Cell. Signal.* 2007. **19**: 844–854.

11 Baker, P., Pettitt, A., Slupsky, J., Chen, H., Glenn, M., Zuzel, M. and Cawley, J., Response of hairy cells to IFN-alpha involves induction of apoptosis through autocrine TNF-alpha and protection by adhesion. *Blood* 2002. **100**: 647–653.

12 Chen, Q., Gong, B., Mahmoud-Ahmed, A., Zhou, A., Hsi, E., Hussein, M. and Almasan, A., Apo2L/TRAIL and Bcl-2-related proteins regulate type I interferon-induced apoptosis in multiple myeloma. *Blood* 2001. **98**: 2183–2192.

13 Chawla-Sarkar, M., Leaman, D. and Borden, E., Preferential induction of apoptosis by interferon (IFN)-beta compared with IFN-alpha2: correlation with TRAIL/Apo2L induction in melanoma cell lines. *Clin. Cancer Res.* 2001. **7**: 1821–1831.

14 Kayagaki, N., Yamaguchi, N., Nakayama, M., Eto, H., Okumura, K. and Yagita, H., Type I interferons (IFNs) regulate tumor necrosis factor-related apoptosis-inducing ligand (TRAIL) expression on human T cells: A novel mechanism for the antitumor effects of type I IFNs. *J. Exp. Med.* 1999. **189**: 1451–1460.

15 Yanase, N., Hata, K., Shimo, K., Hayashida, M., Evers, B. and Mizuguchi, J., Requirement of c-Jun NH2-terminal kinase activation in interferon-alpha-induced apoptosis through upregulation of tumor necrosis factor-related apoptosis-inducing ligand (TRAIL) in Daudi B lymphoma cells. *Exp. Cell Res.* 2005. **310**: 10–21.

16 de Weerd, N. A., Samarajiwa, S. A. and Hertzog, P. J., Type I interferon receptors: biochemistry and biological functions. *J. Biol. Chem.* 2007. **282**: 20053–20057.

17 Nagata, S., Apoptosis by death factor. *Cell* 1997. **88**: 355–365.

18 Griffith, T., Chin, W., Jackson, G., Lynch, D. and Kubin, M., Intracellular regulation of TRAIL-induced apoptosis in human melanoma cells. *J. Immunol.* 1998. **161**: 2833–2840.

19 Wiley, S. R., Schooley, K., Smolak, P. J., Din, W. S., Huang, C. P., Nicholl, J. K., Sutherland, G. R. *et al.*, Identification and characterization of a new

member of the TNF family that induces apoptosis. *Immunity* 1995. **3**: 673–682.

20 **Pitti, R. M., Marsters, S. A., Ruppert, S., Donahue, C. J., Moore, A. and Ashkenazi, A.,** Induction of apoptosis by Apo-2 ligand, a new member of the tumor necrosis factor cytokine family. *J. Biol. Chem.* 1996. **271**: 12687–12690.

21 **Secchiero, P., Melloni, E., Heikinheimo, M., Mannisto, S., Di Pietro, R., Iacone, A. and Zauli, G.,** TRAIL regulates normal erythroid maturation through an ERK-dependent pathway. *Blood* 2004. **103**: 517–522.

22 **Pfeffer, L. M., Dinarello, C. A., Herberman, R. B., Williams, B. R., Borden, E. C., Bordens, R., Walter, M. R. *et al.*,** Biological properties of recombinant alpha-interferons: 40th anniversary of the discovery of interferons. *Cancer Res.* 1998. **58**: 2489–2499.

23 **Williams, B.,** Transcriptional regulation of interferon-stimulated genes. *Eur. J. Biochem.* 1991. **200**: 1–11.

24 **Pfeffer, L., Kim, J., Pfeffer, S., Carrigan, D., Baker, D., Wei, L. and Homayouni, R.,** Role of nuclear factor-kappaB in the antiviral action of interferon and interferon-regulated gene expression. *J. Biol. Chem.* 2004. **279**: 31304–31311.

25 **Du, Z., Wei, L., Murti, A., Pfeffer, S., Fan, M., Yang, C. and Pfeffer, L.,** Non-conventional signal transduction by type 1 interferons: the NF-kappaB pathway. *J. Cell. Biochem.* 2007. **102**: 1087–1094.

26 **Zhang, F. and Sriram, S.,** Identification and characterization of the interferon-beta-mediated p53 signal pathway in human peripheral blood mononuclear cells. *Immunology* 2009. **128**: e905–e918.

27 **Panaretakis, T., Hjortsberg, L., Tamm, K., Bjorklund, A., Joseph, B. and Grander, D.,** Interferon alpha induces nucleus-independent apoptosis by activating extracellular signal-regulated kinase 1/2 and c-Jun NH2-terminal kinase downstream of phosphatidylinositol 3-kinase and mammalian target of rapamycin. *Mol. Biol. Cell* 2008. **19**: 41–50.

28 **Takaoka, A., Hayakawa, S., Yanai, H., Stoiber, D., Negishi, H., Kikuchi, H., Sasaki, S. *et al.*,** Integration of interferon-alpha/beta signalling to p53 responses in tumour suppression and antiviral defence. *Nature* 2003. **424**: 516–523.

29 **Kirou, K., Vakkalanka, R., Butler, M. and Crow, M.,** Induction of Fas ligand-mediated apoptosis by interferon-alpha. *Clin. Immunol.* 2000. **95**: 218–226.

30 **Crowder, C., Dahle, Ø., Davis, R., Gabrielsen, O. and Rudikoff, S.,** PML mediates IFN-alpha-induced apoptosis in myeloma by regulating TRAIL induction. *Blood* 2005. **105**: 1280–1287.

31 **Herzer, K., Hofmann, T., Teufel, A., Schimanski, C., Moehler, M., Kanzler, S., Schulze-Bergkamen, H. and Galle, P.,** IFN-alpha-induced apoptosis in hepatocellular carcinoma involves promyelocytic leukemia protein and TRAIL independently of p53. *Cancer Res.* 2009. **69**: 855–862.

32 **Papageorgiou, A., Dinney, C. and McConkey, D.,** Interferon-alpha induces TRAIL expression and cell death *via* an IRF-1-dependent mechanism in human bladder cancer cells. *Cancer Biol. Ther.* 2007. **6**: 872–879.

33 **Sleijfer, S., Bannink, M., Van Gool, A., Kruit, W. and Stoter, G.,** Side effects of interferon-alpha therapy. *Pharm. World Sci.* 2005. **27**: 423–431.

34 **Ronnblom, L., Alm, G. and Eloranta, M.,** Type I interferon and lupus. *Curr. Opin. Rheumatol.* 2009. **21**: 471–477.

35 **Sedger, L. M., Glaccum, M. B., Schuh, J. C., Kanaly, S. T., Williamson, E., Kayagaki, N., Yun, T. *et al.*,** Characterization of the *in vivo* function of TNF-alpha-related apoptosis-inducing ligand, TRAIL/Apo2L, using TRAIL/Apo2L gene-deficient mice. *Eur. J. Immunol.* 2002. **32**: 2246–2254.

36 **Laird, P. W., Zijderveld, A., Linders, K., Rudnicki, M. A., Jaenisch, R. and Berns, A.,** Simplified mammalian DNA isolation procedure. *Nucleic Acids Res.* 1991. **19**: 4293.

37 **Uze, G., Lutfalla, G. and Gresser, I.,** Genetic transfer of a functional human interferon alpha receptor into mouse cells: cloning and expression of its cDNA. *Cell* 1990. **60**: 225–234.

38 **Domanski, P., Witte, M., Kellum, M., Rubinstein, M., Hackett, R., Pitha, P. and Colamonici, O.,** Cloning and expression of a long form of the beta subunit of the interferon alpha beta receptor that is required for signaling. *J. Biol. Chem.* 1995. **270**: 21606–21611.

39 **Mizushima, S. and Nagata, S.,** pEF-BOS, a powerful mammalian expression vector. *Nucleic Acids Res.* 1990. **18**: 5322.

40 **Shiraishi, T., Suzuyama, K., Okamoto, H., Mineta, T., Tabuchi, K., Nakayama, K., Shimizu, Y. *et al.*,** Increased cytotoxicity of soluble Fas ligand by fusing isoleucine zipper motif. *Biochem. Biophys. Res. Commun.* 2004. **322**: 197–202.

41 **Rubinstein, S., Familletti, P. and Pestka, S.,** Convenient assay for interferons. *J. Virol.* 1981. **37**: 755–758.

Abbreviation: **Oas:** 2′-5′-oligoadenylate synthetase

Correspondence: Prof. Shigekazu Nagata, Department of Medical Chemistry, Kyoto University Graduate School of Medicine, Yoshida-Konoe, Sakyo, Kyoto 606-8501 Japan
Fax: +81-75-753-9446
e-mail: snagata@mfour.med.kyoto-u.ac.jp

Senior editor: Dr. Kohki Kawane, Institut de Biologie du Développement de Marseille-Luminy, UMR 6216 – Case 907, Parc Scientifique de Luminy, 13288 Marseille Cedex 09, France

See accompanying Commentary:
http://dx.doi.org/10.1002/eji.201040829

Received: 21/4/2010
Revised: 5/6/2010
Accepted: 10/6/2010
Accepted article online: 9/7/2010

THE JOURNAL OF BIOLOGICAL CHEMISTRY VOL. 285, NO. 39, pp. 30214–30223, September 24, 2010

Essential Role of p400/mDomino Chromatin-remodeling ATPase in Bone Marrow Hematopoiesis and Cell-cycle Progression*[S]

Received for publication, January 15, 2010, and in revised form, June 3, 2010 Published, JBC Papers in Press, July 7, 2010, DOI 10.1074/jbc.M110.104513

Toshihiro Fujii (藤井俊裕)[‡§], **Takeshi Ueda** (上田健)[§1], **Shigekazu Nagata** (長田重一)[‡§¶], **and Rikiro Fukunaga** (福永理己郎)[‡§¶2]

From the [‡]Department of Medical Chemistry, Graduate School of Medicine, Kyoto University, Yoshida-Konoe, Sakyo-ku, Kyoto 606-8501, the [§]Graduate School of Frontier Biosciences, Osaka University, Osaka 565-0871, and the [¶]Core Research for Evolutional Science and Technology, Japan Science and Technology Corporation, Saitima 332-0012, Japan

p400/mDomino is an ATP-dependent chromatin-remodeling protein that catalyzes the deposition of histone variant H2A.Z into nucleosomes to regulate gene expression. We previously showed that p400/mDomino is essential for embryonic development and primitive hematopoiesis. Here we generated a conditional knock-out mouse for the p400/mDomino gene and investigated the role of p400/mDomino in adult bone marrow hematopoiesis and in the cell-cycle progression of embryonic fibroblasts. The Mx1-Cre- mediated deletion of p400/mDomino resulted in an acute loss of nucleated cells in the bone marrow, including committed myeloid and erythroid cells as well as hematopoietic progenitor and stem cells. A hematopoietic colony assay revealed a drastic reduction in colony-forming activity after the deletion of p400/mDomino. Moreover, the loss of p400/mDomino in mouse embryonic fibroblasts (MEFs) resulted in strong growth inhibition. Cell-cycle analysis revealed that the mDomino-deficient MEFs exhibited a pleiotropic cell-cycle defect at the S and G_2/M phases, and polyploid and multinucleated cells with micronuclei emerged. DNA microarray analysis revealed that the p400/mDomino deletion from MEFs caused the impaired expression of many cell-cycle-regulatory genes, including G_2/M-specific genes targeted by the transcription factors FoxM1 and c-Myc. These results indicate that p400/mDomino plays a key role in cellular proliferation by controlling the expression of cell-cycle-regulatory genes.

The alteration of chromatin structure and function is a critical process in the transcriptional activation or repression of various cell-type-specific or developmentally regulated genes and is mainly executed by covalent histone modification and ATP-hydrolysis-dependent chromatin remodeling. All of the ATP-dependent chromatin remodelers are multisubunit protein complexes containing a SWI2/SNF2 family ATPase subunit, which plays a central role in chromatin-remodeling activities (1, 2). p400/mammalian Domino (p400/mDomino,[3] Gene symbol: *Ep400*), which was identified as an interaction partner for adenovirus E1A (3) and a myeloid-specific transcription factor, MZF-2A (4), is an SWR1-class chromatin-remodeling ATPase that is homologous to the yeast Swr1p and *Drosophila* Domino proteins (5, 6). The p400/mDomino-containing protein complex consists of more than 10 subunits, including the Tip60 histone acetyltransferase and a PI3K family protein kinase TRRAP (3, 7, 8). The SWR1-class remodelers are responsible for the regulated exchange of selective histone H2A variants, such as H2A.Z, with the canonical H2A in nucleosomes (5, 9–11). This histone-exchanging activity plays a key role in the epigenetic regulation of gene expression as well as in DNA repair (12–16).

p400/mDomino is known to interact physically and/or functionally with growth-regulating transcription factors, such as Myc, p53, E2F, and adenovirus E1A (3, 17–20). In primary human fibroblasts and osteosarcoma-derived U2OS cells, the knockdown of p400/mDomino results in cell-cycle arrest at the G_1 phase with the induction of p21 expression (21, 22). At the p21 promoter, p400/mDomino colocalizes with p53 at a p53-binding site and with c-*myc* at a TATA region to regulate p21 expression (16, 19). Thus, p400/mDomino appears to regulate both the p53-dependent and c-Myc-modulated expression of p21, which blocks cell proliferation and leads to cellular senescence. However, a recent study showed that the siRNA-mediated knockdown of p400/mDomino in mouse cells reduces the proliferation rate of embryonic stem cells without p21 up-regulation, and has only a modest effect on the cell cycle of embryonic fibroblasts (23). This discrepancy in the effect of p400 knockdown on cellular proliferation could be attributable to cell-type-specific roles of p400/mDomino, or different levels of residual p400/mDomino protein might have resulted in the distinct phenotypes in these knockdown experiments.

We previously reported that mice with an N-terminally deleted p400/mDomino mutation die *in utero* with a defect in primitive erythropoiesis, indicating that the mDomino complex is essential for early development (24). In this study, we

* This work was supported in part by grants-in-aid from the Ministry of Education, Culture, Sports, Science and Technology of Japan.
[S] The on-line version of this article (available at http://www.jbc.org) contains supplemental Figs. 1 and 2 and Table 1.
[1] Present address: Campbell Family Institute for Breast Cancer Research, Princess Margaret Hospital, Toronto, Ontario M5G 2C1, Canada.
[2] To whom correspondence should be addressed: Dept. of Medical Chemistry, Graduate School of Medicine, Kyoto University, Yoshida-Konoe, Sakyo-ku, Kyoto 606-8501, Japan. Tel.: 81-75-753-9444; Fax: 81-75-753-9446; E-mail: rfukunaga@mfour.med.kyoto-u.ac.jp.

[3] The abbreviations used are: mDomino, mammalian Domino; MEF, mouse embryonic fibroblast; pI:pC, poly(I):poly(C); SPB, sodium phosphate buffer; ER, estrogen receptor; OHT, 4-hydroxytamoxifen; CreER, a fusion of protein Cre with the estrogen receptor; BM, bone marrow; TRRAP, transformation/transactivation domain-associated protein.

generated conditional knock-out mice to examine the role of p400/mDomino in adult mice. The induced deletion of mDomino in mice led to lethality within 2 weeks, accompanied by the rapid loss of bone marrow cells, including hematopoietic progenitor/stem cells. Analysis of the cell-cycle profile of the mDomino-deleted fibroblasts showed that mDomino was essential for cell-cycle progression. Gene expression analysis revealed that the mDomino deletion caused the reduced expression of cell-cycle-regulatory genes that are targets of the transcription factors FoxM1 and c-Myc. These results indicated that mDomino plays a key role in cellular proliferation by regulating the expression of genes involved in cell-cycle progression.

EXPERIMENTAL PROCEDURES

Construction of Targeting Vectors and Generation of Conditional Knock-out Mice—FLPe transgenic mice (25) were kindly provided by Dr. S. Itohara (Brain Science Institute, RIKEN, Japan) through the RIKEN BioResource Center (Tsukuba, Japan). *E2a-Cre* (26) and *Mx1-Cre* transgenic mice (27) were from the Jackson Laboratory. A targeting vector was constructed in which exon 15 of the *mDomino* gene was flanked with two *loxP* sites (Fig. 1*A*). In brief, a *loxP* site was inserted into intron 14, and an *FRT*- and *loxP*-flanked neomycin-resistance gene (*NeoFRT* cassette) was inserted into intron 15 of the *mDomino* gene. The diphtheria toxin A fragment gene (*DTA* cassette) for negative selection was ligated to the 3′-end of the 3′-homologous arm.

$mDom^{+/NeoFRT}$ mice were produced as described previously (28). In brief, mouse R1 embryonic stem (ES) cells were transfected with the targeting vector by electroporation, and G418-resistant clones were screened for homologous recombination by PCR. ES clones carrying the single *mDomino*-targeted allele were injected into BDF1 blastocysts, which were then implanted into recipient ICR female mice. Chimeric mice with a high ES contribution were crossed to C57BL/6 females to yield $mDom^{+/NeoFRT}$ mice. Germ line transmission was identified by coat color and then confirmed by PCR. To remove the NeoFRT cassette, $mDom^{+/NeoFRT}$ heterozygotes were crossed with CAG-FLPe transgenic mice (25), generating $mDom^{+/fl}$ mice. To delete the $mDom^{fl}$ allele *in vivo*, poly(I):poly(C) (pI:pC, BD Biosciences) was given by one intraperitoneal injection (5 mg/kg body weight) every other day, for a total of three injections. All the mice were housed in a specific pathogen-free facility at Kyoto University, and all animal experiments were carried out in accordance with protocols approved by Kyoto University (Kyoto, Japan).

Genomic DNA for PCR was prepared from tail snips. The genotype of the *mDomino* gene was determined by PCR using a mixture of three specific primers: an exon-14 sense primer (5′-ATTGGAAAATCCAACACCAAGGA-3′) and two antisense primers for the wild-type (WT) exon 15 (5′-GTCTCGGAGA-GCACCATACAACAAAGATGG-3′) and its floxed allele (5′-CCCTGGGATGCCTGCAAGCTTATAACTTCG-3′).

For Southern hybridization, genomic DNA extracted from parental and $mDom^{+/NeoFRT}$ ES cells was digested with restriction enzymes, separated by agarose gel electrophoresis, and transferred to a BA85 nitrocellulose filter (Schleicher & Schuell). Hybridization was carried out using a ^{32}P-labeled probe (Fig. 1*A*).

Flow Cytometry and Western Blotting—For flow cytometric analyses, antibodies against the following proteins were purchased from BD Pharmingen: CD3 (145–2C11), CD4 (L3T4), CD8 (53–6.7), c-Kit (2B8), Sca-1 (D7), Mac-1 (M1/70), B220 (RA3–6B2), Gr-1 (RB6–8C5), FcRII/III (2.4G2), Ter119, and CD71 (C2). The flow cytometric characterization of bone marrow hematopoietic cells was performed as described before (29).

To detect endogenous mDomino protein, mouse embryonic fibroblasts (MEFs) were lysed directly in Laemmli sample loading buffer and heated for 30 min at 85 °C and for 5 min at 95 °C. The samples were separated by electrophoresis on a 5% SDS-polyacrylamide gel and transferred to a polyvinylidene difluoride membrane filter (Millipore). Immunoblotting analysis was carried out using the enhanced chemiluminescence system (Millipore) with a rabbit anti-Dom-C polyclonal antibody (4) and peroxidase-conjugated goat anti-rabbit immunoglobulin (Dako).

Histology—To prepare bone marrow sections, femurs were fixed with 4% paraformaldehyde in 0.1 M sodium phosphate buffer (pH 7.2, SPB) containing 4% sucrose, and then incubated at room temperature for 24 h in Morse's solution (0.4 M sodium citrate and 22.5% formic acid) for decalcification, and embedded in paraffin. The blocks were sectioned at 4 μm, deparaffinized, and subjected to staining with hematoxylin and eosin.

To detect apoptotic cells, tissues were fixed in 0.1 M SPB containing 4% sucrose and 4% paraformaldehyde at 4 °C for 2 h, then transferred to 0.1 M SPB containing 10% sucrose at 4 °C for 4 h, and then to 0.1 M SPB containing 20% sucrose at 4 °C overnight. The fixed tissues were embedded in OCT compound (Sakura), quickly frozen, sectioned at 8 μm, and mounted onto APS-coated glass slides (Matsunami). For TUNEL staining, the fixed sections were stained with an ApopTag fluorescein *in situ* apoptosis detection kit from Chemicon International, and the nuclei were counterstained with DAPI. The sections were mounted with Fluoromount (Calbiochem) and were visualized by fluorescence microscopy (Keyence BIOREVO).

Cell Culture and Establishment of CreER MEFs—Primary $mDom^{fl/fl}$ MEFs were prepared from E13.5 embryos and immortalized according to the 3T3 protocol. The MEFs were maintained in Dulbecco's modified Eagle's medium supplemented with 10% fetal bovine serum (FBS), 100 units/ml penicillin, and 100 μg/ml streptomycin (hereafter "culture medium") in a humidified atmosphere. The pMXs-CreER^{T2}-IRES-EGFP-puro^{R} plasmid (CreER refers to a fusion of protein Cre with the estrogen receptor) was transfected into the packaging cell line Plat-E (30) using FuGENE transfection reagent (Roche Diagnostics), and the transfected cells were cultured for 2 days to produce a helper-free retrovirus encoding CreER^{T2}. The culture supernatant was recovered and used directly as a retrovirus stock. Immortalized MEFs (1×10^5 cells) in 10-cm dishes were infected by adding 10 ml of the culture medium containing 10 μg/ml Polybrene and 1% of the retrovirus stock. To delete the $mDom^{fl}$ allele from $mDom^{fl/fl}$:*CreER* MEFs, the cells were treated with 7.5 nM 4-hydroxytamoxifen (OHT) for 8 h, washed with the culture medium, and further incubated in

culture medium under a humidified atmosphere. To establish MEFs expressing exogenous *mDomino*, the *mDom*$^{fl/fl}$*;CreER* MEFs were transfected with the pNEF-DomHA plasmid encoding a neomycin-resistance gene and the C-terminally HA-tagged mDomino cDNA (1/2-disrupted Myc-mDomino-HA (4)) by electroporation using the Amaxa system (Amaxa), and stable transfectants were selected by G418 resistance.

Cell-cycle Analysis—Cells were trypsinized and fixed in 70% ethanol overnight at −20 °C, treated with 100 μg/ml RNase A (Sigma) in phosphate-buffered saline (PBS) for 30 min at room temperature, and then incubated with 40 μg/ml propidium iodide in PBS for 30 min on ice. Data were acquired using a FACSCalibur (BD Biosciences) and analyzed using Flow-Jo software (TreeStar, Inc.).

Microarray Analysis—For DNA microarray analysis, RNA was extracted from *Dom*$^{fl/fl}$*;CreER* MEFs that were left untreated or treated with 7.5 nM OHT for 8 h and then cultured for 2 days. Biotin labeling of complementary RNA was performed using the GeneChip 3′ IVT Express kit (Affymetrix). The biotinylated RNA was fragmented and hybridized to Mouse Gene 430 2.0 chips (Affymetrix) as per the manufacturer's protocol. Both raw image (.dat) and intensity (.cel) files were generated using Gene Chip Operating Software (Affymetrix). All the data, including the signal intensity of each gene, were determined with Microarray Analysis Suite Version 5.0 (Affymetrix). The overall signal intensity of each array was normalized so that the average would be 500. The -fold change analysis was done using the average of OHT-untreated MEFs (n = 3) relative to the average of OHT-treated MEFs (n = 3). p values were calculated using Student's t test. The data were filtered for a change in expression exceeding 2.0-fold and a p value of <0.015. In addition, in the assessment of down-regulated genes, genes presenting with a negative value in at least one of the three profiles or with an average intensity of <100 were deleted in the profiles of OHT-untreated MEFs.

Real-time PCR for the Quantitative Analysis of mRNA—For the reverse-transcribed (RT)-PCR reaction, cDNA was synthesized from DNase I-treated total RNA (0.5 μg) using an oligo(dT) primer and Superscript III (Invitrogen) in a 10-μl reaction mixture. Quantitative real-time RT-PCR was carried out using the LightCycler 480 SYBR Green system (Roche Diagnostics), as described before (31), under the following conditions: 10 s at 95 °C, 10 s at 60 °C, and 20 s at 72 °C for 40 cycles. The primer sets used were: 5′-AGCGTTAAGCAGGAACTGGA-3′ and 5′-TCTGCTGTGATTCCAAGTGC-3′ for FoxM1, 5′-TCACTTCTGGCTACATCCCC-3′ and 5′-ATAGGACTCCGTGCCATCAC-3′ for PLK1, 5′-TGAGGAGAAGCAGTGAGGAA-3′ and 5′-CTGAGAGGTATTCTTAGCCT-3′ for CENP-F, 5′-GGGAGAACTTTCCAGGTGTC-3′ and 5′-AGAGAGACTCATCGAGCGAG-3′ for Skp2, 5′-GTGGGTCAGCGCCACACCTC-3′ and 5′-GGGAGAGGCGCTTGTGCAGG-3′ for p53, 5′-TGGCTGGCGGTAAGGCTGGA-3′ and 5′-ACGTCCGTGGCTGGTTGTCC-3′ for H2A.Z, 5′-GGACTGTATGTGGAGCGGTT-3′ and 5′-GAATCGGACGAGGTACAGGA-3′ for c-Myc, and 5′-CCCAGCGCCTGGCCTATGTG-3′ and 5′-TGCAGTCCGGTCCTCCCCAG-3′ for E2F1. All the PCR data were normalized to standards and expressed as copy numbers of target mRNA per nanogram of total RNA.

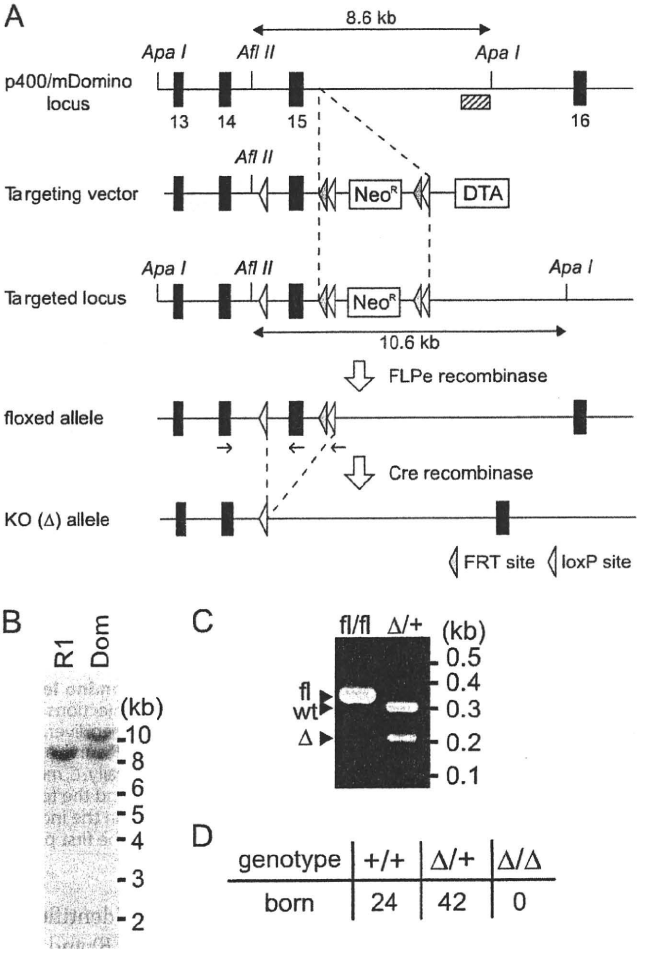

FIGURE 1. **p400/mDomino is essential for embryonic development.** *A*, schematic illustration of the exon organization of the p400/mDomino gene and targeting strategy. A targeting vector was designed in which exon 15 was flanked by two loxP sites, and an *FRT/loxP*-flanked Neo cassette (*NeoFRT*) was inserted into intron 15. Removal of the *NeoFRT* cassette by FLPe recombinase generated the *mDom*^{fl} allele. Cre-mediated recombination between the loxP sites generated the exon-15-deleted allele (*mDom*$^{\Delta}$). The positions of the primers used for genotyping are indicated by *short arrows*. *B*, Southern blot analysis of a correctly targeted ES clone. Genomic DNA from parental (*R1*) or targeted (*Dom*) ES cells was digested with ApaI and AflII, and analyzed by Southern blotting using the probe indicated by the *hatched box* in *A*. The WT and targeted mDom alleles were predicted to result in 8.6- and 10.6-kb bands, respectively, as shown in *A*. *C*, PCR genotyping of *mDom*$^{fl/fl}$ and *mDom*$^{\Delta/+}$ mice. *D*, genotype analysis of the progeny from *mDom*$^{\Delta/+}$ heterozygous matings.

RESULTS

Generation of p400/mDomino Conditional Knock-out Mice—The targeting construct that was designed to delete exon 15 of the *mDomino* gene by Cre-mediated recombination is shown in Fig. 1*A*. The deletion of exon 15 from the *mDomino* locus is expected to remove the catalytic center of the ATPase domain and to generate a mutant mDomino that lacks a major portion (encoded by exons 15–52) of the protein (4). We used an *FRT*- and *loxP*-flanked Neo cassette (*NeoFRT*) and a DTA cassette as positive and negative selection markers, respectively, for homologous recombination. Mouse ES cell clones containing

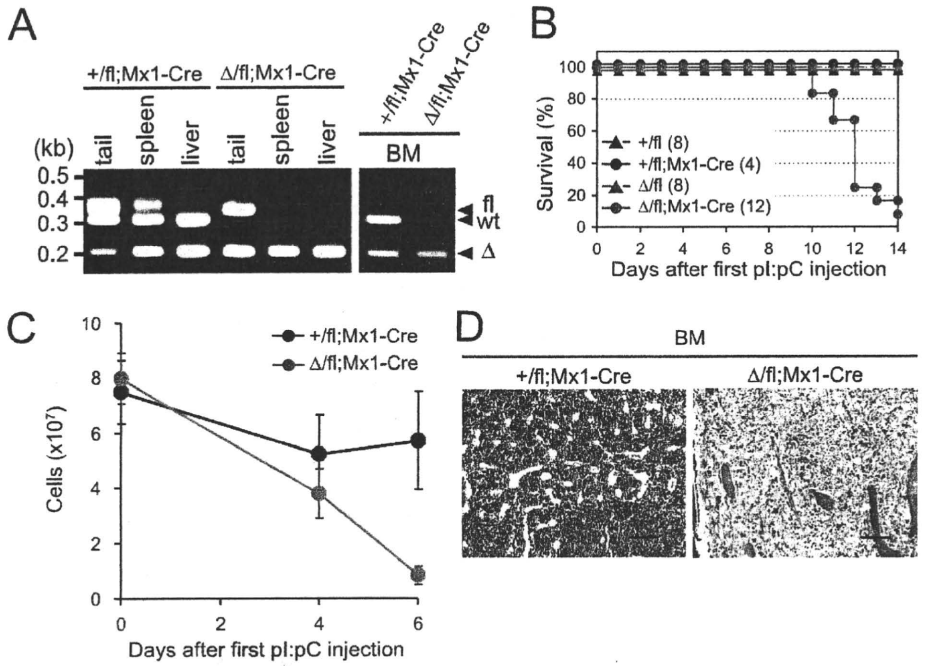

FIGURE 2. **Mx1-Cre-mediated conditional deletion of mDomino leads to rapid mortality and a loss of bone marrow cells.** Mice were given three intraperitoneal injections of pI:pC, one each on days 0, 2, and 4, and then analyzed. *A*, PCR genotyping of DNA from the tail, spleen, liver, and BM was performed on day 6 for the pI:pC-treated $mDom^{+/fl}$;*Mx1-Cre* and $mDom^{\Delta/fl}$;*Mx1-Cre* mice. *B*, survival of the pI:pC-treated $mDom^{\Delta/fl}$;*Mx1-Cre* mice ($n = 12$) and control mice ($n = 20$ in total) was observed daily. *C*, $mDom^{+/fl}$;*Mx1-Cre* mice (*black*, $n = 3$) and $mDom^{\Delta/fl}$;*Mx1-Cre* mice (*red*, $n = 3$) were treated with pI:pC, and the total number of nucleated BM cells in all the femurs and tibiae from a single mouse was determined on the indicated days. *D*, hematoxylin and eosin staining of a paraffin-fixed section of the femur 8 days after the first pI:pC injection. *Scale bars* represent 100 μm.

the *mDomino*-targeted allele ($mDom^{NeoFRT}$) were identified by PCR (not shown) and Southern blot analyses (Fig. 1*B*) and were used to generate mice carrying the $mDom^{NeoFRT}$ allele in the germ line. Then, the $mDom^{NeoFRT}$ mice were crossed with *CAG-FLPe* transgenic mice (25) to remove the *NeoFRT* cassette. The resulting *mDomino* allele containing two *loxP* sites in introns 14 and 15 (the "floxed" allele) was designated as $mDom^{fl}$ (Fig. 1, *A* and *C*). $mDom^{fl/fl}$ mice were obtained from heterozygous matings at a Mendelian ratio and were phenotypically indistinguishable from their wild-type (WT) or heterozygous littermates, indicating that the $mDom^{fl}$ allele was functional (data not shown). We also crossed $mDom^{NeoFRT}$ mice with *E2a-Cre* transgenic mice (26), to obtain an *mDomino* allele lacking exon 15 in the germ line, which was designated as $mDom^{\Delta}$ (Fig. 1, *A* and *C*). Heterozygous $mDom^{\Delta/+}$ mice were born and developed normally, but no homozygous mutant offspring were born from the intercross of $mDom^{\Delta/+}$ mice, indicating that the homozygous $mDom^{\Delta/\Delta}$ mutation is lethal during embryonic development (Fig. 1*D*). We have not determined whether $mDom^{\Delta/\Delta}$ embryos die in a very early stage of embryogenesis, or can develop at least to embryonic day 8.5 as observed in the homozygous embryos expressing the N-terminally deleted mDomino mutant (24).

Acute Loss of Bone Marrow Hematopoietic Cells Caused by the Induced Deletion of mDomino—To generate mice in which the *mDomino* gene was inducibly inactivated, $mDom^{fl}$ mice were crossed with *Mx1-Cre* transgenic mice (*Mx1-Cre*), which carry the Cre gene under the control of the Mx1 promoter. The *Mx1-Cre* gene is induced in adult mice by the administration of poly(I):poly(C) (pI:pC) via interferon (IFN) induction (27). To estimate the efficiency of the *mDom* deletion in adult tissues, pI:pC was administered intraperitoneally to *mDom-floxed* mice three times, once each on days 0, 2, and 4. Two days after the last pI:pC injection, genomic DNA from the tail, spleen, liver, and bone marrow (BM) was analyzed by PCR. Although the deletion of the floxed exon 15 of the $mDom^{fl}$ allele was inefficient in the tail, an efficient deletion of the floxed allele (50–70%) was observed in the spleen, and almost complete deletion was achieved in the liver and BM in the $mDom^{\Delta/fl}$;*Mx1-Cre* and the $mDom^{+/fl}$;*Mx1-Cre* mice (Fig. 2*A*).

To explore the role of mDomino in adult mice, $mDom^{\Delta/fl}$;*Mx1-Cre* mice were injected with pI:pC, as described above. This treatment resulted in the death of almost all of the $mDom^{\Delta/fl}$;*Mx1-Cre* mice within 14 days after the first pI:pC injection, whereas no mortality was observed in any of the pI:pC-injected control mice ($mDom^{+/fl}$; Mx1-Cre, $mDom^{\Delta/fl}$, and $mDom^{+/fl}$) (Fig. 2*B*). Our previous study showed that mice with the N-terminally deleted mDom mutation die during embryonic development with defects in primitive hematopoiesis (24). Therefore, to investigate the roles of mDomino in adult hematopoiesis, we examined the BM phenotypes of the pI:pC-injected $mDom^{\Delta/fl}$;*Mx1-Cre* mice on days 4 and 6 (*i.e.* 0 and 2 days after the last pI:pC injection, respectively), and found a drastic reduction of nucleated cells (Fig. 2*C*). Hematoxylin-eosin staining revealed the obvious disappearance of BM hematopoietic cells, except for the anucleate mature erythrocytes (Fig. 2*D*). These results indicated that the proliferation and maintenance of hematopoietic cells in the BM are severely impaired by the inactivation of mDomino.

To determine which of the BM hematopoietic lineages was affected by the mDomino deficiency, we analyzed the BM cells of pI:pC-treated $mDom^{\Delta/fl}$ mice by flow cytometry. The treatment of control mice, such as $mDom^{+/fl}$;*Mx1-Cre* mice (Fig. 3, *A* and *B*) and $mDom^{\Delta/fl}$ mice (free of *Mx1-Cre*, data not shown), with pI:pC resulted in a significant reduction of bone marrow $B220^+$ B cells and $Ter119^+$ erythroid cells but not of $Mac\text{-}1^+$ or $Gr\text{-}1^+$ myeloid cells, indicating that IFN (and/or pI:pC itself) has some deleterious effect on the lymphoid and erythroid lineages but not on the myeloid lineage. In contrast, the deletion of mDomino in BM cells resulted in a significant reduction of the $Mac\text{-}1^+Gr\text{-}1^{mid\text{-}lo}$ monocyte/macrophage lineage and $Mac\text{-}1^+Gr\text{-}1^{hi}$ granulocyte lineage (Fig. 3, *A* and *B*). The $CD71^+Ter119^{mid\text{-}hi}$ erythroid progenitors were also dimin-

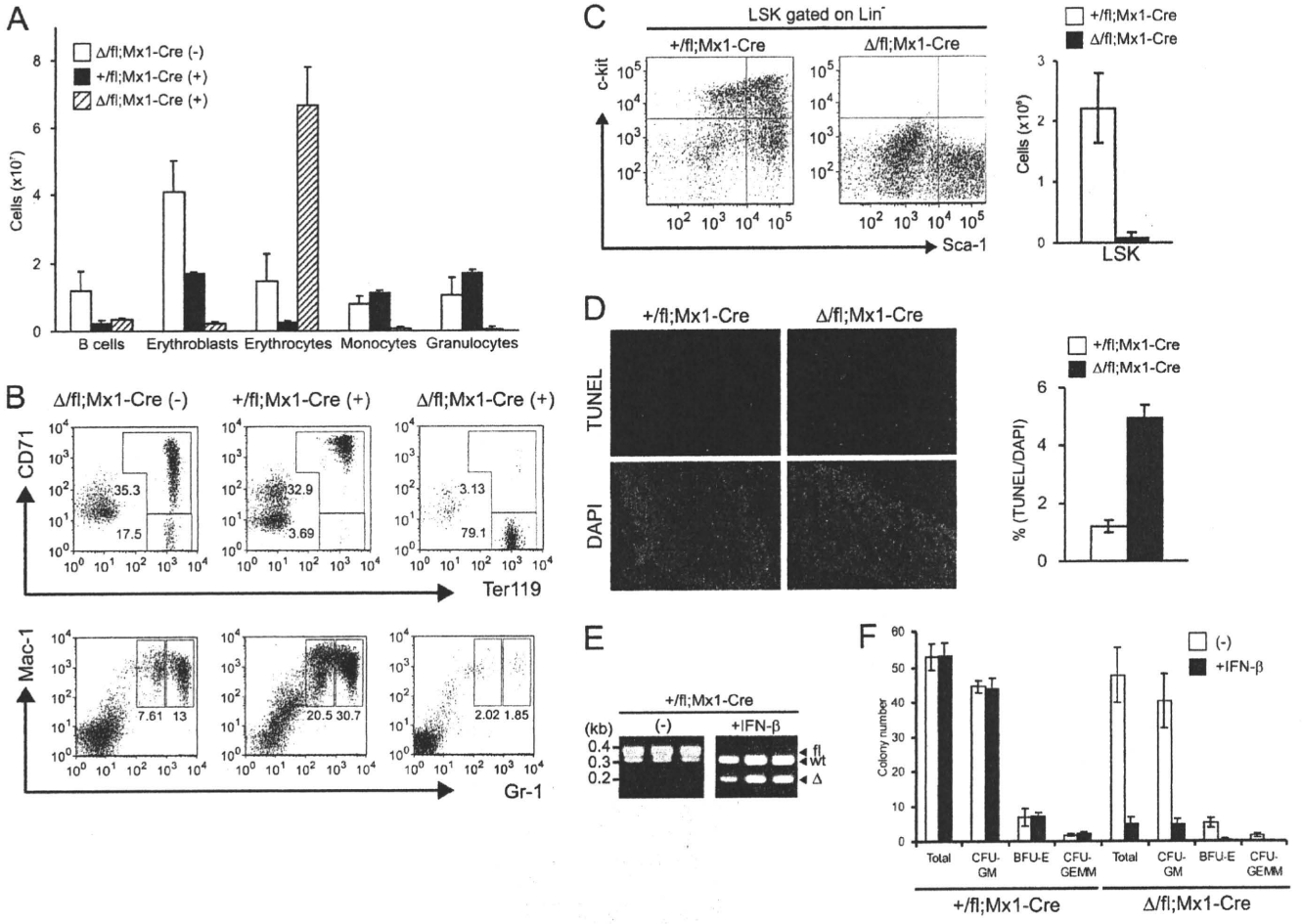

FIGURE 3. **Loss of BM hematopoietic cells by mDomino deletion.** *A*, total number of BM hematopoietic subsets ($n = 3$, mean ± S.E.) in pI:pC-treated (+) or untreated (−) mice on day 4. The number of cells in each subset was calculated from the total number of nucleated BM cells and the flow cytometric analysis of hematopoietic subsets shown in *B*. The hematopoietic subsets were defined by lineage markers as follows: B cells ($B220^+$), erythroblasts ($CD71^{hi}Ter119^{mid}$ and $CD71^{lo\text{-}hi}Ter119^{hi}$), erythrocytes ($CD71^-Ter119^{hi}$), monocytes ($Mac\text{-}1^+Gr\text{-}1^{mid}$), and granulocytes ($Mac\text{-}1^+Gr\text{-}1^{hi}$). *B*, flow cytometric profiles of BM cells from pI:pC-treated (+) or untreated (−) mice on day 4. *C*, flow cytometric analysis of lineage-marker-negative (Lin^-) hematopoietic stem and progenitor cells (*left*), and the total number of $Lin^-Sca\text{-}1^+c\text{-}Kit^+$ (LSK) stem cells (*right*) among the BM cells from pI:pC-injected mice. *D*, apoptotic cell death in the mDomino-deleted BM cells. Cryosections of BM were prepared from pI:pC-injected mice on day 3. The BM samples were stained with TUNEL and counterstained with DAPI (*left*). The TUNEL-positive cells were counted, and the percentage of DAPI-positive cells that were TUNEL-positive was calculated (*right*). *E* and *F*, *in vitro* hematopoietic colony assay of $mDom^{\Delta/fl}$;*Mx1-Cre* BM cells under the induced deletion of mDomino by IFN-β. BM cells (2×10^4 nucleated cells) from $mDom^{+/fl}$;*Mx1-Cre* or $mDom^{\Delta/fl}$;*Mx1-Cre* mice were cultured using the MethoCult M3434 system (Stem Cell Technologies) in 35-mm culture dishes in the presence or absence of 100 units/ml mouse IFN-β (Merck), in duplicate. *E*, three colonies from each of the IFN-treated or untreated (−) cultures of $mDom^{+/fl}$;*Mx1-Cre* BM cells were analyzed for mDomino deletion by PCR. *F*, BM cells were cultured in the presence (*filled bars*) or absence (*open bars*) of IFN-β, and colonies of the colony-forming unit (CFU)-GEMM (granulocyte/erythrocyte/macrophage/megakaryocyte) and CFU-GM (granulocyte/macrophage), and the burst-forming unit of erythroid (BFU-E) containing more than 30 cells were counted after 12 days of culture.

ished when compared with the pI:pC-injected control mice. The reduction in nucleated hematopoietic cells was accompanied by a dramatic increase in $CD71^-Ter119^{high}$ mature erythrocytes, which comprised nearly 80% of the non-adherent cells in the BM cavity (Fig. 3, *A* and *B*). Furthermore, lineage-marker-negative (Lin^-)$c\text{-}kit^+Sca\text{-}1^+$ hematopoietic stem cells and $Lin^-c\text{-}kit^+Sca\text{-}1^-$ progenitor cells were lost in the pI:pC-treated $mDom^{\Delta/fl}$;Mx1-Cre mice (Fig. 3C), indicating that mDomino is necessary for the proliferation and/or maintenance of hematopoietic progenitor/stem cells as well as of committed myeloid cells. To address whether the mDomino-deleted hematopoietic cells underwent apoptosis, we analyzed BM cells using the TUNEL assay. One day after the second pI:pC injection, the BM cells from $mDom^{\Delta/fl}$;*Mx1-Cre* mice displayed more TUNEL-positive cells than the control (Fig. 3*D*). Similar results were obtained by immunohistochemical staining for active caspase-3 (data not shown), indicating that the rapid extinction of nucleated hematopoietic cells from the mDom-deleted BM is, at least in part, due to an increase in their apoptotic cell death.

Next, we examined the effect of mDomino deletion on the *in vitro* growth and differentiation of erythroid and myeloid progenitors using a multilineage colony assay. The BM cells from $mDom^{\Delta/fl}$;*Mx1-Cre* mice or control $mDom^{+/fl}$;Mx1-Cre mice were cultured in methylcellulose medium containing multiple cytokines in the presence or absence of IFN-β. The presence of 100 units/ml IFN-β, which effectively deleted the $mDom^{fl}$ allele (Fig. 3*E*), did not have any deleterious effect on the hematopoietic colony formation (CFU-GM, BFU-E, and CFU-GEMM) of control BM cells (Fig. 3*F*, *left*), but resulted in a drastic reduc-